Fakultät für Medizin
II. Medizinische Klinik und Poliklinik

Transgenic T-cells as immunotherapeutics and cell carriers of oncolytic virus for improved cancer treatment

Lisa Magdalena Zeitlinger

Vollständiger Abdruck der von der Fakultät für Medizin der Technischen Universität München zur Erlangung des akademischen Grades eines

Doktors der Medizin (Dr. med.)

genehmigten Dissertation.

Vorsitzender: Prof. Dr. Jürgen Schlegel

Prüfer der Dissertation:

1. apl. Prof. Dr. Oliver Ebert

2. apl. Prof. Dr. Per Sonne Holm

Die Dissertation wurde am 15.05.2018 bei der Technischen Universität München eingereicht und durch die Fakultät für Medizin am 11.12.2018 angenommen.

Abstract

Due to obvious limitations of conventional cancer therapies, oncolytic viruses have emerged as novel alternative agents to specifically target and cause cytolysis of cancer cells. We previously demonstrated that oncolytic vesicular stomatitis virus (VSV), applied via hepatic arterial infusion, results in significant tumor necrosis and survival prolongation in immune-competent rats bearing multifocal, orthotopic HCC. Nevertheless, the systemic delivery of virus faces limited efficacy due to rapid clearance from circulation. The use of cell carriers represents an ideal approach to overcome this challenge, by offering the possibility to shield oncolytic viruses against neutralizing components of the blood and non-specific uptake by circulating immune cells, while simultaneously providing a delivery mechanism through specific homing of the carrier cells to the tumor. In particular, the use of T-cell receptor (TCR) transgenic T-cells to deliver oncolytic viruses to tumors expressing the target antigen is an appealing strategy, as it not only provides tumor specificity in virus delivery and transfer, but the carrier cells themselves possess a direct antitumor effector function, allowing additive or potentially synergistic therapeutic effects with viral therapy.

In this study, we characterized oncolytic VSV and adoptive TCR transgenic T-cell therapy, both alone and in combination, in a model *in vitro* system. We show that human T-cells represent potent carriers for oncolytic VSV, as they allow efficient intracellular replication and transfer of viral progeny to tumor cells. Further, we demonstrate a substantial shielding effect of the virus when incubating infected T-cells with virus-neutralizing serum. In co-cultivation with target tumor cells, we show that VSV-infection of TCR T-cells does not interfere with their antitumor effector functions and leads to increased tumor cell lysis.

Taken together, our results indicate that the use of TCR transgenic T-cells as carriers of oncolytic VSV could provide a potent combination for cancer therapy, by enriching the viral load at the tumor site to optimize the direct oncolytic effect of the virus and simultaneously delivering a powerful immune therapy to target the remaining tumor cells which evade viral infection. Further *in vivo* investigations are warranted in anticipation of a potential clinical application for cancer therapy.

Table of contents

Table of figures

Abbreviations

°C	centigrade
Ab	antibody
BHK-21	baby hamster kidney cell line
CPE	cytopathic effect
FBS	fetal bovine serum
G-MEM	Glasgow Minimal Essential Medium
GFP	green fluorescent protein
h	hour(s)
HCC	hepatocellular carcinoma
IFN	interferon
i.t.	intratumoral
i.v.	intravenous
Luc	Luciferase
mg	milligram
min	minute(s)
ml	milliliter
mm	millimeter
MOI	multiplicity of infection (Ratio of agents to infection targets)
OD	optical density
OV	oncolytic virus
PBMC	peripheral blood mononuclear cells
p.i.	post infection
PBS	phosphate buffered saline
pfu	plaque forming units
RNA	ribonucleic acid
RT	room temperature
rVSV	recombinant VSV
s	second(s)
SD	standard deviation
TAA	tumor-associated antigen
$TCID_{50}$	tissue culture infective dose 50
TCR	T-cell receptor
U	unit(s)
UV	ultraviolet
VSV	Vesicular stomatitis virus
w/o	without
wt	wild-type
µl	microliter

1 Introduction

1.1 Oncolytic Virotherapy

1.1.1 Oncolytic viruses as agents for tumor therapy

Oncolytic viruses (OVs) have emerged as novel alternative agents to specifically target and cause cytolysis of cancer cells, while leaving the healthy surrounding tissue unharmed. Mainly, two different types of OVs can be distinguished: Their tumor selectivity can either be inherent, as for Newcastle disease virus (NDV), vesicular stomatitis virus (VSV) or reovirus, or achieved through genetically engineering, as is the case for adenovirus, herpes simplex virus type 1 (HSV-1) and vaccinia virus. Tumor cells become susceptible to OVs because of defects in the signaling pathways, which occur during malignant transformation. This can be exploited by these viruses and thereby used to support their own replication (Kirn, Martuza et al. 2001, Everts and van der Poel 2005). In particular, in many cancerous cells the type I interferon (IFN) pathway, which is normally responsible for inducing antiviral responses in healthy cells, is impaired (Stojdl, Lichty et al. 2000, Critchley-Thorne, Simons et al. 2009). So, while in normal cells the viral infection is rapidly cleared, OVs can replicate efficiently in tumor tissue.

The concept of using viruses as a weapon against malignant cells is quite old. Already in the early 20th century there was a reported case of a spontaneous remission of tumor after the injection of a live rabies vaccine, leading to the first clinical trial of virotherapy supervised by Nicola De Pace (Power and Bell 2007). During the last decades, in the era of genetic engineering, research in this attractive field gained momentum, and the repertoire of OVs with enhanced potency, specificity and tolerability expanded quickly. Recently, several viral platforms have already found their way into phase one to three clinical trials for evaluating their safety and efficacy. Excitingly, two genetically engineered OVs have already obtained clinical approval. One is the modified adenovirus H101 approved for head and neck cancer in China in 2005 (Garber 2006), and the other is the mutated HSV-1 T-vec (talimogene laherparepvec) for use in advanced melanoma, approved in the U.S. and in Europe in 2015 (Coffin 2016).

1.1.2 Mechanism of action

OVs achieve their antitumor activities through direct and indirect mechanisms:

Direct infection

OVs access their target cells by either binding to surface-receptors or by merging with the plasma membrane. Once the cell is infected, the virus multiplies rapidly within and subsequently leads to lysis of the cell. Infected tumor cells die as a result of competition for metabolic resources, as well as direct, virus-mediated cytotoxicity and cell lysis by massive production and release of viral particles. The viral progeny will then infect surrounding tumor cells leading to amplification of viral therapy (Marchini, Scott et al. 2016).

Vascular rupture

While the direct lytic effect of OV was formerly presumed to be the main mechanism of action, there is growing evidence that the indirect anti-cancer effects are also essential for efficient virotherapy. Some OVs, including the vaccinia virus (Breitbach, Arulanandam et al. 2013) and HSV (Benencia, Courreges et al. 2005), are able to selectively target tumor-associated vasculature. The direct infection of endothelial cells in the tumor microenvironment leads to vascular disruption, thereby compromising the blood flow to the tumor and leading to tumor cell necrosis. In addition to the endogenous ability of targeting tumor endothelial cells, OVs can also be genetically engineered to support the expression of anti-angiogenic factors, which result in a breakdown of tumor neovascularization. Those and other strategies affecting the tumor vasculature have been reviewed in detail (Toro Bejarano and Merchan 2015).

Antitumor immunity

Although the direct killing of cancerous cells and the indirect damage of tumor beds caused by attacking their vasculature are important mechanisms of virotherapy, another crucial aspect of the therapy is the induction of adaptive immune responses directed against the tumor. Especially for VSV, reovirus and HSV, the priming of antitumor immunity has been

demonstrated to have immense relevance to the overall therapeutic efficacy (Diaz, Galivo et al. 2007, Workenhe, Simmons et al. 2014, Gong, Sachdev et al. 2016).

Viral infection leads to the release of cytokines, tumor associated antigens (TAAs) and other danger signals, such as pathogen-associated molecular patterns (PAMPs) and danger-associated molecular patterns (DAMPs). Once the released molecules come into contact with antigen-presenting cells in the tumor microenvironment, such as dendritic cells, a potent immune response can be triggered, causing destruction of not only infected cancerous cells, but also uninfected, surrounding tumor cells (Guo, Liu et al. 2014, Lichty, Breitbach et al. 2014).

1.1.3 Limitations and strategies to improve oncolytic virotherapy

Despite the developments in the field of OV, several challenges remain which limit the full success of virotherapy. In particular, efficient systemic delivery of OVs to the tumor site is one of the major limitations. If administered systemically, e.g. intravenously (i.v.), the virus faces rapid clearance from circulation, due to various factors such as neutralizing antibodies, complement activation, antiviral cytokines, tissue-resident macrophages, and non-specific uptake by liver and spleen (Alemany, Suzuki et al. 2000, Underhill and Ozinsky 2002). Therefore, effective therapies often rely on intratumoral (i.t.) application to ensure the delivery of high titers of virus to the tumor site.

Nevertheless there are several advantages to systemic administration, as not all tumors are accessible to i.t. injection, either because of anatomic circumstances or due to disseminated tumor nodules throughout the body. Therefore, systemic delivery would be the ideal application route to treat metastatic disease (Garnock-Jones 2016, Thomas, Meza-Perez et al. 2016). Several strategies for improvement are currently under investigation, including the use of cell carriers, known as the “Trojan horse” technique, representing an ideal approach to overcome this challenge. In this strategy, carrier cells are isolated from the host, infected *in vitro*, and reapplied systemically. The ideal carrier cells would then traffic to tumor beds and release their viral payload. This technique offers the possibility to shield OV against neutralizing components of the blood and non-specific uptake by circulating

immune cells, as the carriers are initially ignored by the immune system (Power and Bell 2007). Various cell types have already been tested as potential viral carriers, including immune cells such as cytotoxic T-lymphocytes, dendritic cells and macrophages (Roy and Bell 2013), as well as tumor cells themselves, such as myeloma cells, that naturally traffic to the bone marrow (Munguia, Ota et al. 2008).

Beside the use of carrier cells, there are other approaches to shield viruses on their way through the bloodstream. For instance, the utilization of synthetic materials, such as liposome encapsulation (Yotnda, Davis et al. 2004) or by using polymers like polyethylene glycol (PEG) coating the virus (Tesfay, Kirk et al. 2013) have been shown to be effective shielding alternatives. Those strategies help to overcome the rapid clearance of OV in the blood circulation.

Another barrier that needs to be addressed is the relatively inefficient extravasation of OV to the tumor beds. One idea to resolve this problem is to increase the permeability of tumor blood vessels, which can be accomplished by treatment with several agents such as interleukin-2 (IL-2), histamine or a bradykinin analog (Barnett, Rainov et al. 1999, Kottke, Galivo et al. 2008). Another strategy addresses the tumor vessel endothelium where potential targets include VEGF and their receptors, prostate-specific membrane antigen (PSMA), Endoglin or Annexin A2, which are overexpressed on tumor endothelial cells (Neri and Bicknell 2005). The modification of OVs can enable them to target the tumor vasculature by binding to specific receptors (Cattaneo, Miest et al. 2008). Another concept to improve extravasation has been shown with an engineered adenovirus encoding a syncytium-forming protein that triggers fusion of infected endothelial cells and uninfected epithelial cells, permitting transendothelial viral entry (Chen, Cawood et al. 2011).

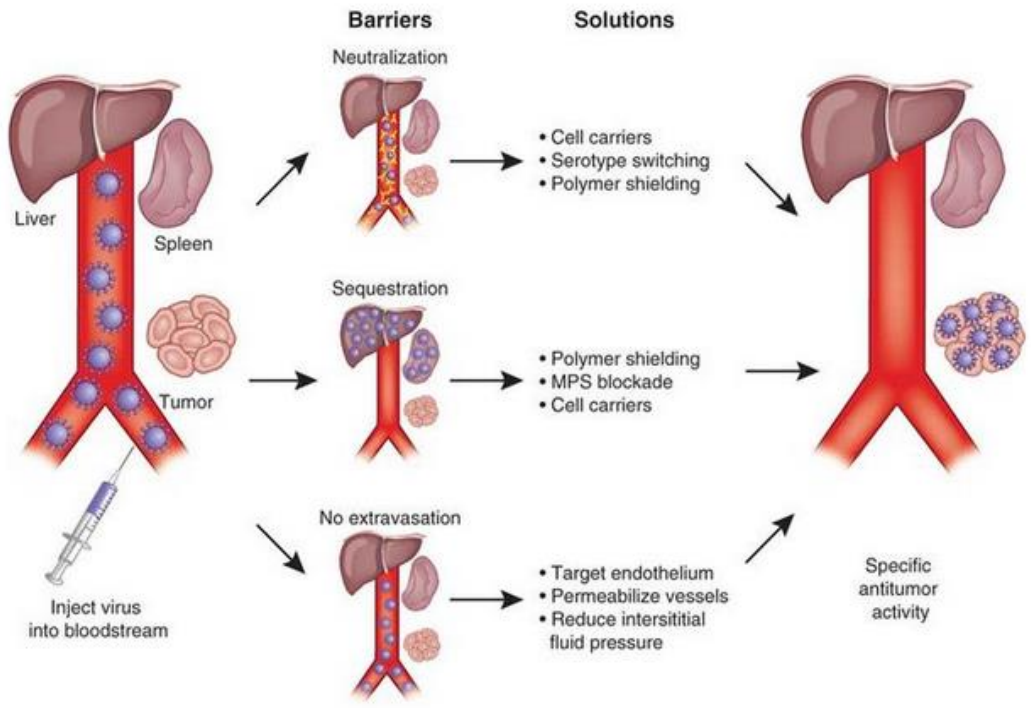

Figure 1: Limitations of virotherapy and alternative strategies to overcome hurdles
(Russell, Peng et al. 2012)

1.2 Vesicular Stomatitis Virus

1.2.1 Characteristics

Vesicular stomatitis virus (VSV) is an enveloped, non-segmented, negative-strand RNA virus and belongs to the Rhabdoviridae family. It is transmitted via insect vectors and is mainly pathogenic to animals. Natural hosts include cattle, pigs and horses, where infections generally lead to fever and blister-like lesions of the oral cavity. VSV rarely infects humans, but if so, infections are usually asymptomatic or manifest as flu-like symptoms. The relatively compact VSV genome contains approximately 11,000 nucleotides encoding for five major proteins. The glycoprotein (G) mediates the cell entry by attaching to receptors of the host cells. The large polymerase (L) protein and phosphoprotein (P) are essential for genome replication. The RNA genome is encapsidated along its entire length by the nucleocapsid (N) protein, and the matrix (M) protein is responsible for the characteristic shape of the

virus and for suppressing antiviral responses through inhibition of host gene expression. The replication of VSV occurs in the cytoplasm of the infected cells. (Lyles and Rupprecht 2007)

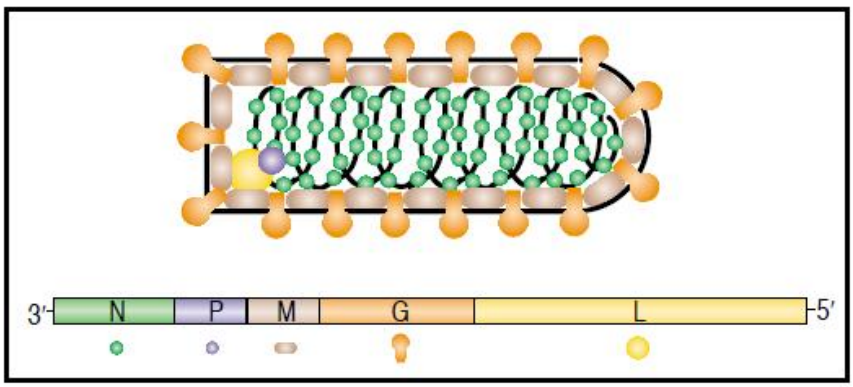

Figure 2: Characteristic structure of vesicular stomatitis virus (VSV) and its genome
The VSV genome encodes five different proteins: the nucleocapsid (N) protein, the phosphoprotein (P), the matrix (M) protein, the glycoprotein (G) and the large polymerase (L) protein. All together they form the characteristic bullet shaped VSV virion. (Lichty, Power et al. 2004)

VSV represents a promising oncolytic agent for cancer therapy as it has inherent tumor specificity due to its extreme sensitivity to the antiviral actions of type I IFN (Critchley-Thorne, Simons et al. 2009). Defects in IFN signaling in tumor cells allows free replication of the virus, while IFN-sensitive, healthy cells are able to protect themselves by inducing an antiviral response. Furthermore, VSV provides some other attractive features for oncolytic virotherapy, including a short replication cycle, rapid tumor cell killing and very low pre-existing immunity in humans. In research, VSV is often used because of its attractive characteristics, like a small genome that can easily be manipulated and the ability to infect a large variety of laboratory cell lines. Moreover, very high virus yields can be achieved easily (Hastie and Grdzelishvili 2012). Despite these beneficial features, one critical disadvantage needs to be addressed: its neurotropism. As wt VSV is able to cross the blood brain barrier, replication in brain and spinal cord is possible and can lead to encephalitis. Thus, many ef-

forts have been made to improve the safety of VSV treatment by reducing the undesirable off-target effects. To overcome the inherent neurovirulence, several new approaches have been tested, including the insertion of IFN-β gene into the VSV genome and the modification of the VSV G protein, which seems to be responsible for its neurotoxic effects, (Jenks, Myers et al. 2010, Hastie, Cataldi et al. 2013).

1.2.2 Use of VSV as treatment for HCC

VSV is already well characterized and shows some promising results in several tumor models. In particular, one of the first reported effective treatments of HCC using VSV was in 2003 by Ebert et al. (Ebert, Shinozaki et al. 2003). This study showed that a single intratumoral application of recombinant VSV results in survival prolongation in immune-competent rats bearing a single nodule, orthotopic HCC compared to buffer treated rats. Next, the VSV therapy was applied via hepatic arterial infusion to HCC-bearing rats with multifocal lesions. Again, similar results could be demonstrated; significant survival benefits were shown, with a median survival time of 36 days for virus treated animals compared to 21 days in control group as seen in Figure 3 (Shinozaki, Ebert et al. 2004). Both studies reported no significant hepatotoxicity associated with the virotherapy.

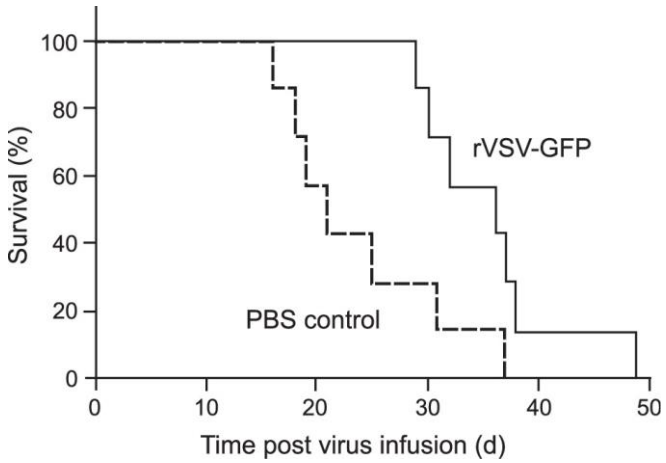

Figure 3: Survival time after VSV treatment of multifocal HCC-bearing rats

Kaplan-Meier curve of multifocal HCC-bearing rats after hepatic arterial injection of either VSV (n=7) or buffer control (n=7). A significant survival benefit could be demonstrated after treatment with recombinant VSV.

Due to the promising results and this unique possibility to apply therapeutic agents locally to liver tumors via hepatic arterial infusion, a detailed protocol was established recently by Altomonte et al. (Altomonte, Munoz-Alvarez et al. 2016). This technique cannot only be used for efficient delivery of OV, but also for other treatment options such as chemotherapy or immune-modulatory drugs.

Over the years, several approaches were investigated for further improvement of efficacy and safety of VSV therapy. For example, a recombinant VSV vector with an inserted fusion protein leads to extensive syncytia formation and therefore enhances the cytotoxic potential (Ebert, Shinozaki et al. 2004). Furthermore, a repeated application of VSV leads to increased tumor necrosis in HCC nodules and survival prolongation of tumor-bearing rats compared to a single injection (Shinozaki, Ebert et al. 2005). Another approach introduces a combination therapy with transarterial embolization (TAE), a well-established treatment option for patients with advanced HCC, which augmented oncolytic effects. The application of viroembolization therapy showed promising results in tumor necrosis and survival prolongation compared to each approach alone (Altomonte, Braren et al. 2008). Regarding safety issues, a recent study demonstrated that the inhibition of a transcription factor (STAT3) reduces virus-induced cytotoxicity in healthy tissues when combined with VSV therapy (Marozin, Altomonte et al. 2015). Another point of interest in recent studies deals with the fate of VSV in fibrotic liver which often underlies clinical onset of HCC in patients. It was shown that recombinant VSV offers antifibrotic properties through several mechanisms, including the specific killing of activated hepatic stellate cells, which promote the degradation of normal matrix and the replacement with fibrotic scar matrix (Altomonte, Marozin et al. 2013).

As a result of this convincing preclinical data about VSV treatment against HCC, a phase I clinical trial was initiated by the Mayo Clinic (NCT01628640) in 2012. A recombinant VSV expressing interferon-beta has recently shown improved safety in Buffalo rats and macaques (Jenks, Myers et al. 2010) and is now used in this trial for treatment of patients with liver cancer. As the patient recruitment and data collection is still ongoing, primary results will be estimated in 2018.

Taken together, several recent studies focus on enhancement of safety and efficacy of VSV therapy that is evolving as a promising therapeutic approach in the treatment of HCC and has high potential for clinical application. Its future development for clinical translation will be exciting to follow.

1.3 Combination therapy for improved virus delivery

1.3.1 T-cells as potential candidates for cell carrier systems

It is speculated that the antiviral immune response limits the full success of oncolytic virotherapy, due to the rapid clearance of the OV from the bloodstream after systemically administration. Therefore the need for effective virus delivery is one of the main ongoing hurdles that still need to be addressed. T-lymphocytes are an appealing class of cells, as they are generally ignored by the immune system while trafficking through the circulation (Power and Bell 2007). In particular, tumor-specific T-cells might be ideal candidates as cell carriers, as they are already under intense investigation for cancer treatment themselves. On the surface of many tumors, there are specific antigens expressed, termed tumor-associated antigens (TAAs) that can be recognized by T-cells, subsequently leading to tumor destruction through the cytotoxic effector functions of the cells. For immunotherapy, those preexisting tumor-reactive cells need to be extensively expanded *in vitro* after being recovered from tumors prior to readministration to the patient. Many preclinical and clinical studies have shown promising results of this so called adoptive immunotherapy (Dudley and Rosenberg 2003).

The use of tumor-specific T-cells as carriers has several benefits to offer: Carrier cells shield the OV against neutralizing blood components or non specific uptake, while providing a specific delivery to the tumor site through homing of the carrier cells to the tumor. Additionally, tumor-specific T-cells themselves possess cytotoxic effector functions, and by employing them as carriers for an OV, synergistic effects could be achieved by combining the direct oncolytic effect with an adoptive immune therapy (Diaz, Galivo et al. 2007, Qiao, Wang et al. 2008).

1.3.2 T-cell receptor (TCR) transgenic T-cells

It has become clear that the effect of naturally-derived tumor-specific T-cells is very limited due to immune tolerance mechanisms within the tumor microenvironment, as well as their TAAs being derived from endogenous tissue (i.e. self-antigens). However, in the era of genetic engineering, the role of T-cells in tumor therapy is constantly evolving. Many strategies focus on generating T-cells that are able to target specific TAAs by inserting genes encoding cell surface receptors, such as T-cell recptors (TCRs) or chimeric antigen receptors (CARs). For this process, T-cells are isolated from a patient's blood and activated and expanded *in vitro*. Subsequently, the generation of TCR transgenic T-cells is generally performed via transduction with replication incompetent viral vectors, including retroviruses and lentiviruses, or alternatively, via plasmids, encoding the TCR (Kershaw, Westwood et al. 2013). Adoptive immunotherapy empolying TCR T-cells has already found its way into clinical trials. Rosenberg et al. reported in 2006, that the infusion of genetically modified lymphocytes, recognizing the melanocyte-differentiating antigen (MART-1), resulted in long-term persistence of administered cells *in vivo* and led to tumor regression in 2 out of 15 patients with metastatic melanoma (Morgan, Dudley et al. 2006). Follow-up studies, using TCRs with higher affinity, again reported promising results in melanoma patients, and for the first time, TCR transduced T-cells were successfully used for treatment in non-melanoma tumors (Johnson, Morgan et al. 2009, Robbins, Morgan et al. 2011). Nevertheless, severe adverse effects limit the full success of T-cell adoptive immunotherapy as a cancer treatment. Especially MART-1-specific, high affinity TCR lymphocytes lead to destruction of normal tissue where melanocytes are present, including skin, eyes and inner ears (Johnson, Morgan et al. 2009). Furthermore, unexpected cross-reactivity to normal tissue caused by TCR transgenic T-cells that have never gone through the thymic checking system, represents a challenge that should not be underestimated (Restifo, Dudley et al. 2012). One of the main hurdles to overcome remains the identification of suitable antigens that are expressed on tumors, but not on healthy tissue in order to minimize off-target toxicity.

For this project, we collaborated with the group of Prof. Angela Krackhardt, who established techniques to generate TCR transgenic T cells against several TAAs in a humanized system (Schuster, Busch et al. 2007, Weigand, Liang et al. 2012, Klar, Schober et al. 2014).

In particular, this group identified myeloperoxidase (MPO) as a novel target antigen expressed by acute myeloid leukemia cells and investigated a TCR construct that recognizes this antigen. For this process, T-cells were isolated from PBMCs and modified with the construct of TCR2.5D6 via retroviral transduction. This TCR demonstrated specific anti-leukemic reactivity *in vitro*, and promising results could be observed in animal experiments, including survival prolongation in mice (Klar, Schober et al. 2014).

1.3.3 Strategy of a hypothesized translational approach

The aim of this project was to combine oncolytic virotherapy with TCR transgenic T-cells into a single therapeutic agent to optimize the positive features of each approach. For translational application, the strategy would include the isolation of T-cells from patient-derived blood, followed by the generation of TAA-specific TCR transgenic T-cells. These cells would be infected *ex vivo* with VSV and systemically re-administered to the patient where they could accomplish their expected goal by delivering and releasing the virus to the tumor site, while also exerting their own cytotoxic effector functions in the cancer cells.

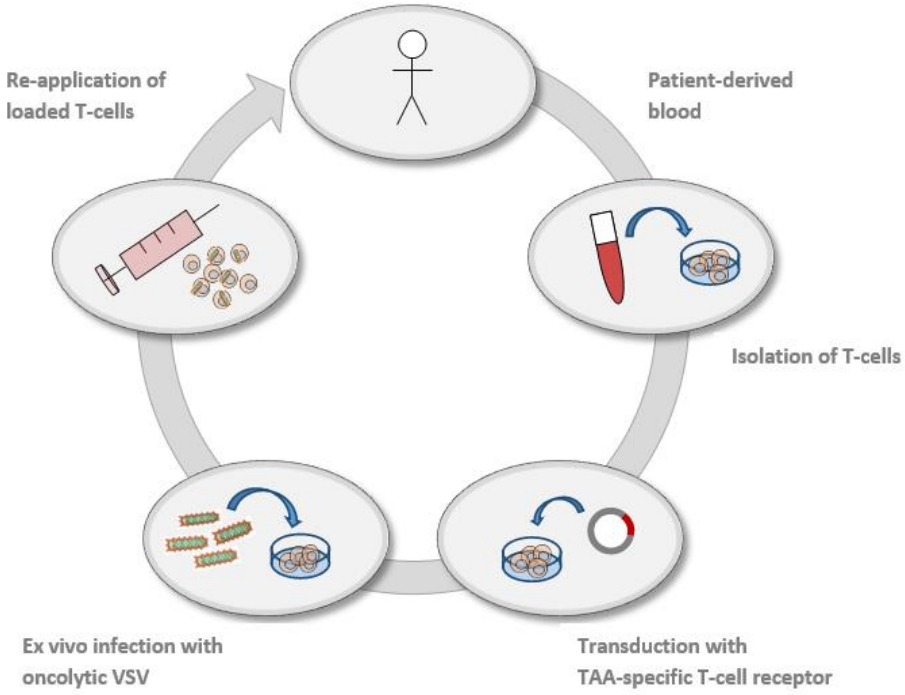

Figure 4: Schematic overview of a proposed translational approach

In order to combine oncolytic virus therapy and adoptive T-cell therapy into a single therapeutic agent, the strategy proposes isolation of T-cells from patient's blood, transduction with an TAA-specific T-cell receptor construct, *ex vivo* infection with oncolytic VSV and re-application of the loaded T-cells to the patient.

1.4 Aim of the work

Due to various hurdles in the delivery of OVs, which limits their capacity to provide an effective cancer therapy, the use of T-cell receptor (TCR) transgenic T-cells offers a novel strategy to overcome this challenge. In particular, TCR transgenic T-cells deliver OVs to tumors expressing the target antigen, which is an appealing concept, as it not only provides tumor specificity in virus delivery and transfer, but the carrier cells themselves possess a direct antitumor effector function, allowing additive or potentially synergistic therapeutic effects with viral therapy.

The aim of this work was to characterize oncolytic VSV and adoptive TCR transgenic T-cell therapies, both alone and in combination, in a model *in vitro* system. Preliminary experiments focused on the VSV infection kinetics and replication properties in human primary T-cells for optimizing the T-cell loading protocol. Next, the effects of VSV on TCR transgenic T-cells were monitored in terms of their function, activation and viability post infection. Finally, the efficacy in tumor cell killing of these therapies was investigated for both modalities, either alone or in combination, in order to reveal potential synergy. In addition, the ability of T-cells to shield VSV from inactivation from neutralizing antibodies was evaluated, as this is an additional crucial benefit of a potential combination therapy.

As a proof of principal, the experiments were performed in a cell line of acute myeloid leukemia cells (AML) that have been transduced with HLA-B7 (ML2-B7) and TCR transgenic T-cells, provided by a collaborating group (Prof. Dr. med. Angela Krackhardt; III. Medizinische Klinik, Klinikum rechts der Isar).

2 Materials and Methods

2.1 Materials

2.1.1 Cells lines, primary cells and viruses

Cell lines	Cell type/ origin	Culture medium
BHK-21	Baby hamster kidney cells	G-MEM BHK-21 + 10% FBS, 1% P/S, 1% TPB
ML2-wt	Acute myeloid leukemia cells	RPMI + 10% FBS, 1% P/S, 1% NEAA, 1% NaPyr, 1% L-Gln
ML2-B7	Acute myeloid leukemia cells transduced with HLA B7	RPMI + 10% FBS, 1% P/S, 1% NEAA, 1% NaPyr, 1% L-Gln
Primary cells		
T-cells	T-lymphocytes from human peripheral blood mononuclear cells (PBMC)	RPMI + 5% FBS, 5% HS, 1% P/S, 1% NEAA, 1% NaPyr, 1% L-Gln, 10 ng/ml h-IL7, 10 ng/ml h-IL15
TCR transgenic T-cells	Primary human T-cells engineered by retroviral transduction; kindly provided from AG Krackhardt	RPMI + 5% FBS, 5% HS, 1% P/S, 1% NEAA, 1% NaPyr, 1% L-Gln, 10 ng/ml h-IL7, 10 ng/ml h-IL15
Viruses	**Transgene**	**Storage**
rVSV-GFP	Engineered green fluorescent protein	-80 °C freezer
rVSV-Luc	Firefly luciferase	-80 °C freezer

2.1.2 Cell culture media, supplements and cytokines

Product	Supplier
Dulbecco's PBS (DPBS) w/o Ca & Mg	PAN Biotech
Dulbecco's PBS (DPBS) with Ca & Mg	PAA cell culture company

G-MEM BHK-21	Gibco life technology
RPMI 1640 (RPMI)	PAN Biotech
Opti-MEM	Gibco life technology
OptiPRO SFM	Gibco life technology
Fetal bovine serum, heat inactivated (FBS)	Biochrom
L-glutamine 200mM (L-Gln)	PAA cell culture company
Non-essential amino acids 100x (NEAA)	PAA cell culture company
Normal human serum (HS)	Millipore
Penicillin and streptomycin 10.000 U/ml each (P/S)	Biochrom
Sodium pyruvate 100mM (NaPyr)	PAA cell culture company
Trypsin-EDTA	PAN Biotech
Tryptose phosphate broth solution (TPB)	Sigma Aldrich Company
Recombinant human interleukin 7 (h-IL7)	PeproTech
Recombinant human interleukin 15 (h-IL15)	PeproTech
Recombinant human interleukin 2 (h-IL2)	PromoKine
Dynabeads® human T-activator CD3/CD28	Life Technologies

2.1.3 FACS antibodies and staining reagents

Antigen	Clone	Host	Conjugated fluorophore	Supplier
Human CD4	RPA-T4	Mouse	V450	BD Biosciences
Human CD8	RPA-T8	Mouse	APC	BD Biosciences
Human CD8	RPA-T8	Mouse	PE	BD Biosciences
Human CD8	RPA-T8	Mouse	PE-Cy7	BD Biosciences
Human CD8	RPA-T8	Mouse	FITC	BD Biosciences
Human CD25	2A3	Mouse	PE	BD Biosciences
Human CD25	M-A251	Mouse	PE-Cy7	BD Biosciences
Human CD3	UCHT1	Mouse	V450	BD Biosciences
FACS staining reagents				
7-AAD				Sigma-Aldrich

Abbreviations: 7-AAD: 7-Aminoactinomycin, APC: Allophycocyanin, PE: R-Phycoerythrin, FITC: Fluorescein-isothiocyanate

2.1.4 Kits and biological reagents

Product	Supplier
Kits	
OptiEIA™ human IFN-γ ELISA set	BD Biosciences
Biological reagents	
Fresh human blood	Kindly donated from various consented healthy male people with no known exposure to VSV
Neutralizing serum from VSV-immunized rats	Provided from Dr. rer. nat. J. Altomonte, AG Ebert
Control serum from non-immunized rats	Provided from Dr. rer. nat. J. Altomonte, AG Ebert

2.1.5 Chemicals and solutions

Product	Supplier
Biocoll separating solution	Biochrom
Blotting grade blocker nonfat dry milk (Milk)	Bio-Rad
Dimethyl sulfoxide (DMSO)	Sigma-Aldrich
Ethanol	Carl Roth
Ethanol 80%	Fischer Scientific
HCL 2 mol/L	Carl Roth
Isopropanol	Klinikum rechts der Isar, Apotheke
Konservierer für Wasserbäder	Carl Roth
Paraformaldehyde (PFA)	Sigma-Aldrich
Phosphate buffered saline (PBS)	Appli Chem
Pursept-FD	Merz
Sodium bicarbonate	Sigma-Aldrich
Sodium carbonate	Merck
Sulforic acid 2 N	Carl Roth
Trypan blue	Carl Roth
Tween 20	Bio-Rad

2.1.6 Equipment and consumables

Product	Supplier
Centrifuge 5415R	Eppendorf
Centrifuge 5702R	Eppendorf
Centrifuge 5810R	Eppendorf
Cryo 1 °C freezing container	Nalgene
Freezer -20 °C	Siemens
Freezer -80 °C	Hera freeze Heraeus
Gallios™ flow cytometer	Beckman Coulter
Ice machine	Ziegra
Incubator Hera Cell 240	Heraeus
Laminar flow Hera Safe S2 hood	Kendro
Laminar flow Hera Safe S1 hood	Kendro
MACS magnets	Milteny Biotec
Magnetic stirrer	Heidolph
Micropipettes	Eppendorf
Microplate reader Multiskan Ex	Thermo Labsystems
Microscope Axiovert 40 CFL	Zeiss
Microscope Optech	Exacta Optech
Multichannel pipette 300	Eppendorf
Multipipette plus M4	Eppendorf
Neubauer counting chamber	Roth
Orbital shaker DUOMAX 1030	Heidolph
pH-meter	WTW
Pipetboy	Eppendorf
Thermomixer compact	Eppendorf
Vortex REAX top	Heidolph
Waterbath	GFL
Aspirating pipette	Greiner Bio-One
Cell culture flask with vented screw (75 cm2)	TPP
Cell culture multiwell plates (6-, 12-, 48- and 96-well)	TPP
Cell culture plates 150 mm	TPP
Cell scraper	TPP
Combitips advanced (1 ml, 5 ml, 10 ml)	Eppendorf

Conical Tubes (15 ml and 50 ml)	BD Falcon
Cryo.S™ PP cryo vials	Greiner Bio-One
Disposable pipetting reservoirs	VWR
FACS tubes 1.4ml U-bottom	Micronic
Filter tips, TipOne	StarLab
Needles (20 G, 27 G and 30G)	Braun
NH4-Heparin monovettes 9ml	Sarstedt
Nunc-Immuno ELISA plates	Thermo Scientific
Parafilm	Roth
Petri dish (100 mm x15 mm)	BD Falcon
Safe lock microcentrifuge tubes (1.5 ml)	Eppendorf
Safe lock microcentrifuge tubes (2 ml)	Sarstedt
Safety-Multifly®-Needle	Sarstedt
Serological pipettes (5 ml, 10 ml, 25 ml and 50 ml)	BD Falcon
Syringe filter (0.22 µm)	TPP
Syringe Luer-Lok sterile (5 ml, 10 ml)	BD Falcon

2.2 Methods

2.2.1 Cell culture

All cells were maintained in their appropriate culture medium as described above (Section 2.1.1) in a humidified atmosphere at 5% CO_2 and 37 °C. For passaging, adherent cells were washed once with PBS, trypsinized, and replated at the appropriate density in fresh medium. Cells in solution were spun down with 500 g for 5 min and resuspended in fresh medium. Mycoplasma PCR was performed regularly in order to rule out contamination.

Cell counting

For cell counting, trypan blue was added 1:1 to the cell suspension and transferred to a Neubauer cell counting chamber. 2 quadrants were counted and the mean value was calculated.

Freezing and recultivation of cells

For freezing, the requested amount of cells was washed, spun down and resuspended in 1 ml FBS with 10% DMSO. Afterwards cells were frozen at -80 °C with -1 °C/min rate of cooling using a cryo freezing container. Frozen cells were subsequently transferred to liquid nitrogen for long-term storage.

For recultivation frozen vials were rapidly thawed at 37 °C, cells were transferred to preheated culture medium, washed once and resuspended for cultivation at the required density.

2.2.2 PBMC Isolation from whole human blood and T-cell enrichment

For the isolation of peripheral blood mononuclear cells (PBMCs), whole human blood was freshly collected from a male donor and mixed with coagulation-inhibiting NH4-Heparin. In a 50 ml centrifuge tube, 12.5 ml of blood were mixed with 22.5 ml of RPMI and then gently layered on 15 ml of Biocoll polysaccharide, serving as density gradient. The tube was centri-

fuged, with slow acceleration and deceleration, at 2100 rpm, RT for 20 min in order to separate the blood components into different layers along the gradient. The PBMC layer was carefully collected using a syringe and washed 3 times in RPMI. The purified PBMCs were seeded in activation media (RPMI supplemented with 5% FBS, 5% HS, 1%P/S, 1% NEAA, 1% NaPyr, 1% L-Gln, 10 ng/ml h-IL7, 10 ng/ml h-IL15, 30 U/ml h-IL2 and CD3/CD28 Dynabeads® at 1:1 cells to beads ratio) at a density of 10^6 cells/ml in order to enrich T-cells. After 2 days, lymphocytes in suspension were separated from adherent monocytes, washed and replated in cultivation medium. T-cells were cultured for at least 5 days after activation before using them for any experiment. Following this protocol, a purity of 80- 85% T-lymphocytes in the population can be achieved.

2.2.3 Virus handling and infection

Viruses were kindly provided by Dr. rer. nat. J. Altomonte, AG Ebert. All experiments including virus infection were performed carefully under biosafety level S2 conditions.

For virus infection, cells were counted, resuspended in 100 to 200 µl PBS with Ca and Mg, and virus was added at different multiplicities of infection (MOIs). After an incubation time of 1 h at RT, cells were thoroughly washed with PBS in order to get rid of the remaining virus in the supernatant and supplemented with the appropriate medium for the experiment.

2.2.4 Tissue culture infectious dose 50 ($TCID_{50}$) assay

In order to quantify the infectious amount of virus in a sample, the tissue culture infectious dose 50 ($TCID_{50}$) assay was performed. BHK-21 cells were seeded in a 96-well plate in their appropriate medium 1 day previous to infection, such that a density of approximately 70% at the time of infection would be reached. On the day of infection, 10-fold serial dilutions of each virus sample was prepared using OptiPRO SFM medium supplemented with L-glutamine, and 100 µl of each dilution were added to four wells of the cells, respectively. After incubation for 2 days, cytopathic effects (CPE) were observed under the microscope, and the $TCID_{50}$/ml value was calculated using the following formula: $TCID50/ml = 10^{-(\log a-((1+b/100)-0,5))} * 10$, where “a” stands for lowest dilution with CPE in all 4 quadruplicates and

"b" for percentage of wells showing CPE in the next lower dilution series to "a". $TCID_{50}$/ml data analysis was carried out using the GraphPad Prism software. Error bars, if existing, represent standard deviations.

2.2.5 Virus growth curve

To examine the replication kinetics of VSV in the tumor cells, 1.25 x 10^5 ML2-wt or ML2-B7 cells per sample were infected with rVSV-Luc at a MOI of 0.01 and 10 for 1 h at RT, washed 3 times with PBS, and provided with 250 µl fresh growth medium per sample. At various time points (0, 6, 12, 24, 48 h post-infection (p.i.)), supernatants were collected, and viral titers were determined by $TCID_{50}$ assay as described above.

2.2.6 Interferon sensitivity assay

To demonstrate the sensitivity of the tumor cells to type I interferon (IFN), 2.5 x 10^5 ML2-wt or ML2-B7 cells were plated in 0.5 ml culture medium/well, and 5 different IFN concentrations (0, 10, 100, 500, 1000 U/ml) were applied in triplicates to the tumor cells, respectively. After incubation overnight at 37 °C, cells were infected with rVSV-Luc at MOI 1 and incubated for another 24 h at 37 °C. On the next day, supernatants were harvested, and viral titers were measured by $TCID_{50}$ assay.

2.2.7 Viral transfer assay

In order to monitor if VSV can be transferred from infected T-cells and replicate in target tumor cells, a viral transfer assay was performed. The experiment was carried out in a 48-well plate with 300 µl culture medium/sample in triplicates. 2 x 10^4 T-cells/sample were infected with rVSV-Luc at MOI 1 for 1 h at RT, washed with PBS, and either cultured alone or co-cultured with tumor cells at a ratio of 1:10. As a control, tumor cells were directly infected with the same amount of virus. After 12 and 24 h p.i., supernatants were harvested, and viral titers were measured by $TCID_{50}$ assay.

2.2.8 Virus protection assay

For investigating a potential shielding effect provided by the candidate carrier cells, a protection assay was carried out. To this end, 10^6 T-cells per sample were infected with rVSV-Luc at a MOI of 10 for 1 h at RT in 100 µl PBS with Ca and Mg and then washed 3 times with PBS. Virus-loaded cells or naked virus were incubated either in 50 µl of heat inactivated neutralizing serum (derived from VSV-immunized rats), control serum or PBS, respectively, for 90 minutes at 37 °C. Afterwards, cells were thoroughly washed, lysed by freezing and thawing 2 times, and then $TCID_{50}$ assays to determine intracellular viral titers were performed with all samples. The experiment was carried out in duplicate samples.

2.2.9 Flow cytometry

To characterize the infection kinetics of T-cells, a fluorescence-activated cell sorting (FACS) assay was performed after infection with rVSV-GFP. 3 x 10^5 untransduced T-cells/sample were infected with different MOIs (0.1, 1, 10) in a volume of 200 µl PBS with Ca and Mg for 1 h at RT. Cells were then centrifuged and resuspended in 250 µl of cultivation medium per sample and cultivated at 37 °C. For uninfected control samples, the same protocol was performed in the presence of PBS without virus. The infection was repeated at various time points, so that all samples could be collected and subjected to FACS analysis at the same endpoint.

For preparation of the FACS analysis, all staining and fixation steps were performed on ice and with 4 °C centrifugation. Cells were spun down, and supernatants were collected and stored for further experiments. Next, the cells were blocked in 50 µl of human serum for 10 min, washed with FACS buffer (PBS + 1% FBS) and then stained with the appropriate amount of antibodies (as shown in the table below) in 50 µl of volume. The samples were incubated for 30 min in the dark, washed once and resuspended in 200 µl 1% PFA for fixation and inactivation of the virus prior to transferring the samples for FACS analysis.

As a positive control for each channel, uninfected T-cells were used for single staining following the same protocol. An antibody against a known antigen in the sample was used for each fluorophore. FITC-labeled anti-CD8 was used for the channel which detects rVSV-GFP

infected samples, and the activation marker, CD25 (PE), was substituted by PE-labeled anti-CD8.

Antibody/Agent	Volume per sample
Antibodies/agents for sample staining	
V450 CD4	1.5 µl
APC CD8	1.5 µl
PE CD25	5.0 µl
7AAD live/dead	0.5 µl
Antibodies/agents for single staining	
V450 CD4	1.5 µl
APC CD8	1.5 µl
PE CD8	1.5 µl
FITC CD8	1.5 µl
7AAD live/dead	0.5 µl

FACS analysis was performed on a Beckmann Coulter Gallios™ flow cytometer, acquiring 10,000 events/sample, and FACS data analysis was carried out by using FlowJo vX.0.7 analysis software.

2.2.10 Interferon-gamma ELISA assay

For detection and quantification of human interferon-gamma by enzyme-linked immunosorbent assay (ELISA), the BD OptiEIA™ human IFN-γ ELISA set was used. The experiment was performed following the manufacturer's instructions, with the exception of the following modifications:

- For coating of the 96-well plate, 50 µl of diluted capture antibodies in coating buffer were pipetted to each well instead of 100 µl.

- For blocking, 1% milk powder in PBS was prepared as blocking buffer instead of using PBS with 10% FBS.

- For preparation of the standard curve, IFN-γ standards were prepared by making a 2-fold serial dilution in T-cell culture medium with 1000 pg/ml as the highest concentration. 50 µl of standard or sample were then added to each well instead of 100 µl.

Biological duplicates of all samples were used, with each sample plated in technical duplicates. The absorbance at 450 nm wavelength with wavelength correction at 540 nm absorbance was measured on a Multiskan EX microplate reader. Data analysis was performed using Excel by plotting the standard curve and calculating the linear equation.

2.2.11 Co-cultivation of VSV-loaded TCR transgenic T-cells with target tumor cells

For showing a potentially synergistic effect in tumor cell lysis when combining transduced T-cells and VSV, a co-cultivation assay was performed. In triplicates, the tumor cells (ML2-B7) were incubated with transduced or untransduced T-cells, either with or without virus (rVSV-Luc) at different effector-to-target ratios. The supernatants were collected after various time points and stored at -80 °C for further analysis. As a control, ML2-wt cells were co-cultured with infected transduced T-cells. In order to improve the protocol, alterations regarding to the infection procedure, effector-to-target ratios and time points were made and described in chapter “Results” more precisely. All infections were made with rVSV-Luc (MOI 0.1 or 1) for 1 h at RT in 100 µl PBS with Ca and Mg, followed by washing of the cells and incubation for 16 h in T-cell-medium or direct transfer to tumor cells, depending on the experiment. Experiments were performed in triplicates; however, for FACS analysis, the cells were combined into one single sample per condition.

For all experiments, flow cytometry analysis of tumor cell viability was performed by following the protocol as described above. ML2-B7 cells could be detected by GFP expression, as they are stably transduced with GFP. FACS antibodies for staining were used as shown in the table:

Antibody/Agent	Volume per sample
Antibodies/agents for sample staining	
V450 CD3	1.5 µl
PE-Cy7 CD25	1.5 µl
7AAD live/dead	0.5 µl
Antibodies/agents for single staining	
FITC CD8	1.5 µl
PE-Cy7 CD8	1.5 µl
V450 CD3	1.5 µl
7AAD live/dead	0.5 µl

FACS analysis was performed on a Beckmann Coulter Gallios™ flow cytometer, acquiring 300,000 events/sample, and FACS data analysis was carried out by using FlowJo vX.0.7 analysis software. For statistical analysis GraphPad Prism was used.

The viral titers of infected samples were measured by $TCID_{50}$ assay. Furthermore, an ELISA assay was performed to quantify IFN-γ production and, therefore, the activation status of the T-cells, according to the description above. Transduced samples were diluted in T-cell culture medium before being used for ELISA assay.

3 Results

3.1 VSV effectively replicates in the target tumor cells

As all experiments were performed in a model of acute myeloid leukemia cells (ML2-wt) and in a cell line transduced with HLA-B7 (ML2-B7), the first step was to determine if the virus can replicate effectively in those tumor cells. Both cell lines were infected with VSV at different MOIs, and supernatants were harvested after various time points in order to measure the viral titers. The results show that VSV replicates efficiently, with a peak in titers at around 10^8 $TCID_{50}$/ml, already reached after 24 h (Figure 5). Regardless of whether the tumor cells were infected with a low (MOI 0.01) or high (MOI 10) amount of virus, similar titers were achieved. The replication kinetics demonstrate rapidly increasing titers starting as early as 6 h p.i., whereas after 48 h a slight decrease in titers was observed, which most likely is a reflection of loss of viability of the tumor cells. Growth curves were nearly identical in both cell lines, indicating that expression of HLA-B7 does not influence the susceptibility of ML2 cells to VSV replication. As VSV is replicating effectively in the target tumor cells, further experiments in this model are justifiable.

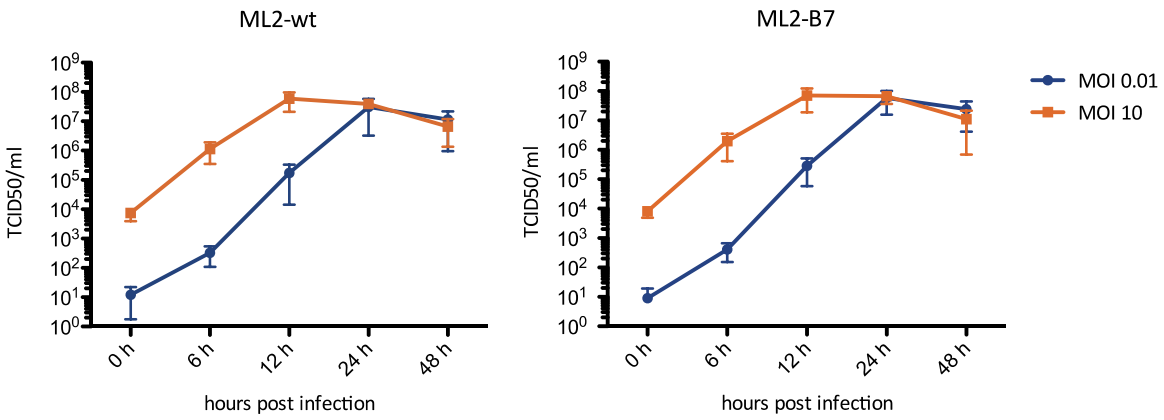

Figure 5: Growth curves showing replication kinetics of VSV in target tumor cells

Viral titers in the supernatants of ML2-wt and ML2-B7 cells after infection with VSV at different MOIs (0.01, 10) got measured after various time points (0, 6, 12, 24 and 48 h p.i.). Virus yields rapidly increase to a maximum of around 10^8 $TCID_{50}$/ml no matter if tumor cells got infected with small or large amounts of virus, showing that further experiments using this model are possible. Data are representative of four individual experiments for ML2-wt cells and three experiments for ML2-B7 cells. $TCID_{50}$/ml is plotted in log scale and values are expressed as mean + SD.

3.2 Target tumor cells are not sensitive to type I interferon

Oncolytic viruses replicate preferentially in tumor cells due to defects in the signalling pathways that occur during malignant transformation. In many cancerous cells the type I interferon pathway, which normally induces an antiviral response, is impaired and the virus can replicate freely. In order to examine this effect, tumor cells were pretreated with different dilutions of type I interferon, infected with VSV at MOI 1, and after an incubation time of 24 h at 37 °C, viral titers in supernatants were measured by $TCID_{50}$ assay. The results show that high viral titers could be achieved regardless of pretreatment with interferon. The addition of lower concentrations of IFN had negligible effects on virus titers, with virus yields of over 10^7 $TCID_{50}$/ml, while at higher concentrations (> 500U/ml), a slight reduction in titer could be observed (Figure 6). No difference between the cell lines could be seen, indicating that retroviral transduction has no major impact on interferon signaling in these cells. Taken together, pretreatment with interferon failed to protect the target tumor cells, indicating that ML2-wt and ML2-B7 cells lost their responsiveness to type I interferon and therefore become susceptible to the virus.

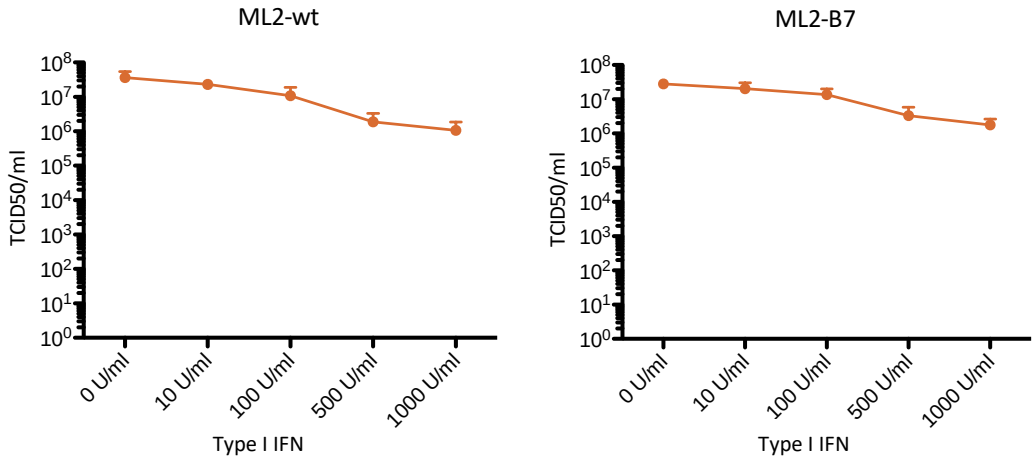

Figure 6: Response of target tumor cells to type I IFN

ML2-wt or ML2-B7 cells were pretreated with 5 different concentrations of IFN (0, 10, 100, 500, 1000 U/ml) overnight, infected for 1 h at 37 °C with rVSV-Luc at an MOI 1 and incubated in fresh medium for another 24 h at 37 °C. Viral titers of supernatants were measured by $TCID_{50}$ assay. Data are representative of five individual experiments for ML2-wt cells and three experiments for ML2-B7 cells. $TCID_{50}$/ml is plotted in log scale, and values are expressed as mean + SD.

3.3 Untransduced human T-cells support productive infection with VSV expressing GFP

Several experiments to characterize T-cells in response to infection with oncolytic VSV virus were performed in order to monitor the infection kinetics, their viability and functionality. For preliminary experiments, untransduced T-cells derived from PBMCs isolated from human blood were used. After activation of PBMCs with CD3/CD28 Dynabeads in combination with human IL2 and cultivation for 5 days, a working cell population with approximately 80-85% $CD4^+$ and $CD8^+$ T-lymphocytes was achieved. Those cells got infected with a recombinant VSV-GFP, containing the green fluorescent protein (GFP) coding sequence that serves as a reporter gene for virus replication in FACS analysis. For an optimized infection protocol, 3 x 10^5 untransduced T-cells/sample were infected with different concentrations of virus (MOI 0.1, 1, 10) in a small volume of serum-free buffer for one hour. Afterwards, cells were washed and cultured in complete medium for 16, 24, 36 or 48 hours and then subjected to further analysis, including FACS analysis to monitor infectibility and viability of the T-cells, while supernatants were kept for ELISA assay to determine the functionality.

For FACS analysis, cells were stained with fluorophore-conjugated antibodies against T-cell markers, CD4 and CD8, the T-cell activation marker, CD25, and 7AAD live/dead staining. Uninfected T-cells (MOI 0) were used as control samples. All samples were fixed in 1% PFA to inactivate the virus prior to analyzing.

The results indicate that untransduced T-cells are susceptible to infection with rVSV-GFP in a time- and dose-responsive manner (Figure 7). GFP positive, living cells (Quadrant Q1) were already detected at 16 h p.i., with an increasing percentage from 1% at MOI 0.1 to 17% and 27.5% at MOI 1 and 10, respectively. At 24 h p.i., the highest percentage of infected living cells could be detected at MOI 1 with 30.6%, while MOI 10 resulted in 18.8%. At the low MOI of 0.1, the peak of GFP positive, living cells could be reached after 36 h p.i. with 17.9%. After 48 h post infection, a drastic decrease in Q1 cells to 3.7%, 2.7% and 1.9% at MOI 0.1, 1 and 10, respectively could be seen. At this late time point the frequency of dead cells has raised to a very high percentage over 60% for all virus concentrations. Furthermore, at MOI 10, the high numbers of cells in the dead fraction could be observed over all time-points, from around 30% at an early time point up to 68% after 48 hours. The inci-

dence of GFP positive, living cells, as well as the increase of dead cells over time and MOI, is summarized in Figure 8A and B and represents an overview of all three individual experiments, highlighting the inter-donor variations among them. Although the same protocol was used for all experiments, the results vary in their infection levels. However, the time- and dose-responsive manner of infection was consistent among all of them, with the highest percentage of GFP+, living cells after treatment at MOI 1 for 24 hours (17.4% to 35.6%) and at MOI 10 at 16 h p.i. (18.1% to 40.7%). Further, we observed that higher levels of infected cells at early time-points lead to a larger population of dead T-cells at following time-points.

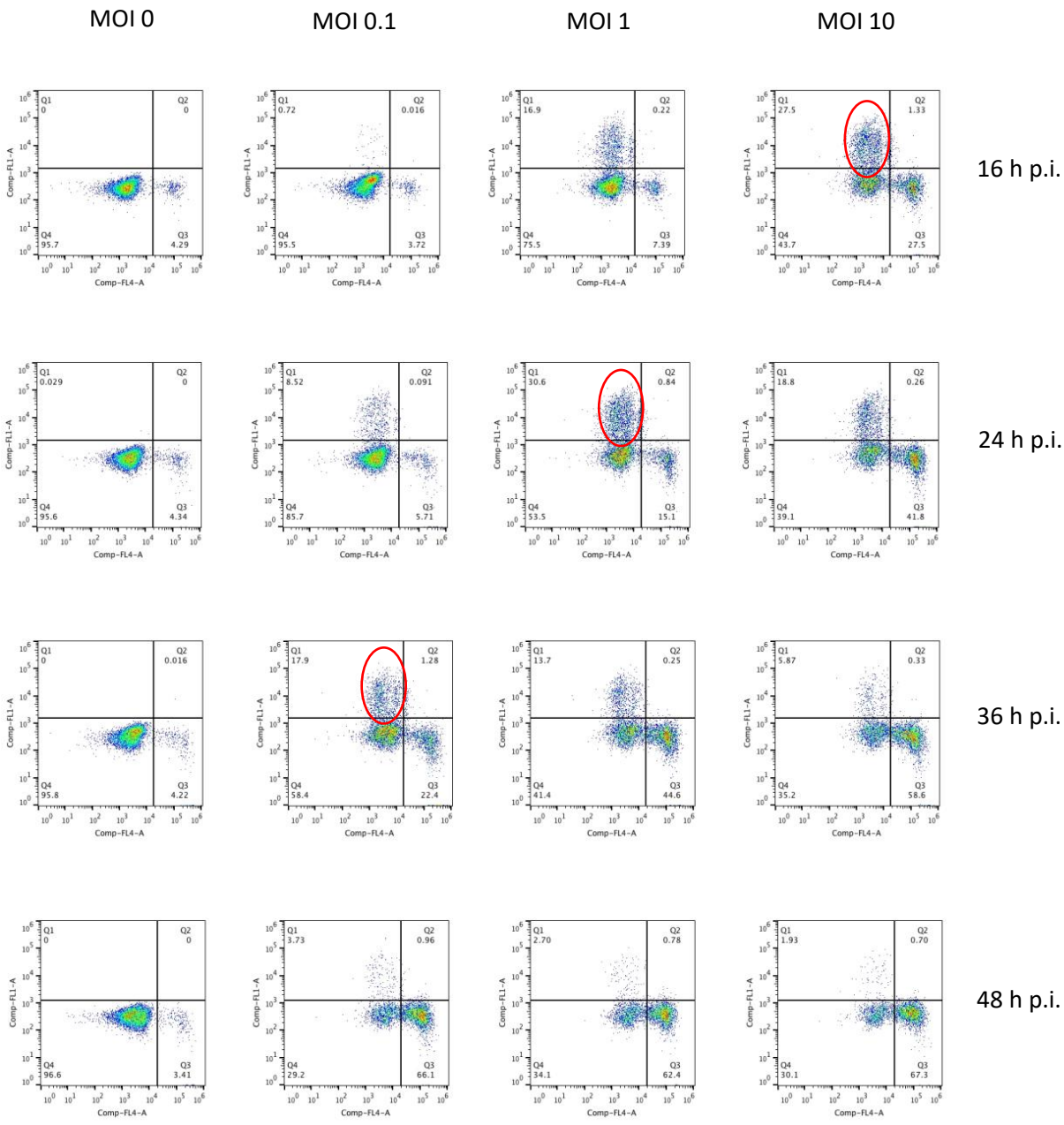

Figure 7: Kinetics of rVSV-GFP infection in untransduced human T-cells

FACS analysis of T-cell samples. T-cells were infected with rVSV-GFP at different MOIs (0.1, 1, 10) for 1 h, washed and incubated in complete medium for 16, 24, 36 or 48 hours. Pseudocolor dot plots of different T-cell samples, gated for lymphocytes by forward and sideward scatter. GFP signal is shown on Y axis (Comp-FL1-A), signal from 7AAD dead cell staining on X axis (Comp-FL4_5-A). Gates and percentages of the full population are shown for all quadrants Q1-Q4. Both axes are plotted in log scale. Data are representative for one out of three reproducible experiments. Red circles highlight the biggest population of infected, living T-cells for each time point.

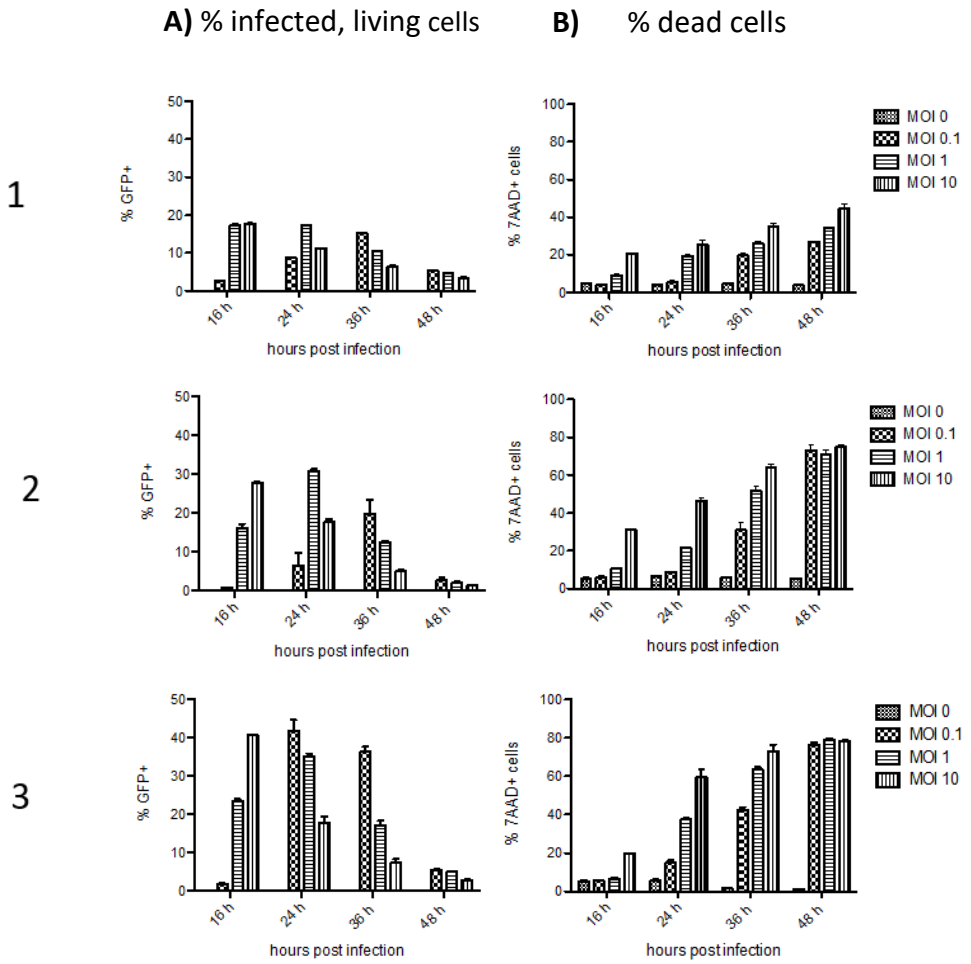

Figure 8: Overview of three independent experiments showing inter-donor variations in terms of infection efficacy

FACS analysis of T-cell samples. T-cells were infected with rVSV-GFP at different MOIs (0.1, 1, 10) for 1 h, washed and incubated in complete medium for 16, 24, 36 or 48 hours. **A)** Frequency of GFP positive cells of the 7AAD negative (living) cell population (Y-axis) is plotted over time (X-axis) for different MOIs. **B)** Frequency of 7AAD positive (dead) cells from the lymphocyte gate (Y-axis) is plotted over time (X-axis) for different MOIs. Mean and SD of two duplicates per sample are plotted.

The supernatants of the infected T-cell samples were subjected to further analysis for activation status by ELISA assay (Figure 9A) and for analysis of viral titers by $TCID_{50}$ assay (Figure 9B).

Analysis of the IFN-γ ELISA assay revealed a linear increase of IFN-γ concentration in supernatants of uninfected control T-cells (MOI 0) from approximately 100 pg/ml up to around 300 pg/ml over time. The same trend could be observed for infected T-cell samples. After

48 hours, IFN-γ levels increased to around 280 pg/ml, 250 pg/ml and 200 pg/ml for MOI 0.1, 1 and 10, respectively. Compared to uninfected cells, IFN-γ concentrations for higher MOIs are slightly reduced, which might be due to a reduction of viable cells to produce IFN-γ. As a positive control, cells were freshly reactivated with CD3/CD28 beads overnight, which resulted in values of over 1200 pg/ml of IFN-γ in the supernatant. Our results suggest that the rVSV-GFP infection does not significantly alter the activation status of the T-cells.

Furthermore, viral titers in the supernatants of rVSV-GFP infected T-cells were determined by $TCID_{50}$ assay. For the lowest infection dose of MOI 0.1, viral titers increased with time from around 5 x 10^5 $TCID_{50}$/ml at 16 h p.i. to 5 x 10^7 at later time points. Higher MOIs show a constant $TCID_{50}$/ml value between 10^7 and 5 x 10^7 over all time points without any significant changes. However, after 48 hours a slight decrease, especially in MOI 10, could be observed.

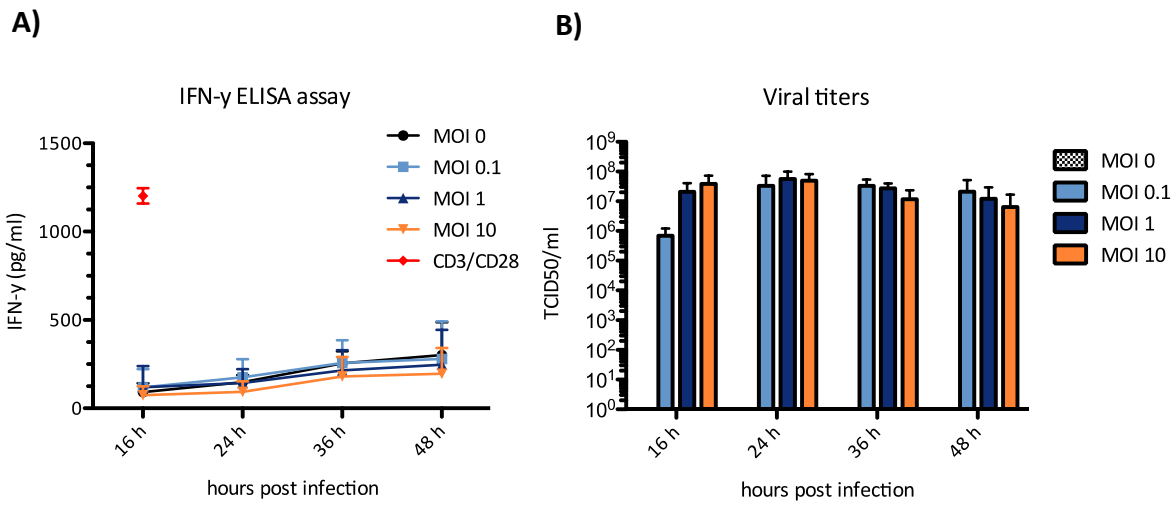

Figure 9: Analysis of infected T-cell supernatant for INF-γ and viral titers

A) Supernatants obtained from T-cells infected with rVSV-GFP were subjected to INF-γ ELISA assay. Concentration of IFN-γ in pg/ml (Y-axis) is plotted as a function of time post-infection (X-axis) for different MOIs. As a positive control, an uninfected sample was reactivated with CD3/CD28 beads overnight. **B)** TCID50 analysis of viral titers in the supernatant of rVSV-GFP infected T-cells (Y-axis) at different time points (X-axis). $TCID_{50}$/ml is plotted in log scale, and values are expressed as mean and SD. Data are representative for three individual experiments with T-cells derived from different donors.

3.4 T-cells protect VSV from neutralizing antibody inactivation

To investigate a potential shielding effect provided by the candidate carrier cells, a protection assay was carried out. 10^6 T-cells per sample were infected with rVSV-Luc at an MOI of 10 for 1 hour, and afterwards, virus-loaded cells or naked virus were incubated with heat inactivated neutralizing serum (derived from VSV-immunized rats), control serum (serum from non-immunized rats) or PBS, respectively. After lysing the cells by repetitive freezing and thawing, a $TCID_{50}$ determination of intracellular viral titers was performed. As a positive control, samples of naked virus were subjected to the same procedure prior to measuring viral titers. As seen in Figure 10, similar intracellular titers could be achieved whether the loaded T-cells were incubated with neutralizing serum, control serum or PBS. Viral titers range from around 10^4 $TCID_{50}$/ml to 10^5 $TCID_{50}$/ml. The VSV-loaded T cells incubated with neutralizing serum demonstrate a reduction of intracellular viral titers by approximately one log compared to control samples. On the other hand, total inactivation of VSV was observed in the naked virus sample after incubation with neutralizing serum. Control samples of naked virus produced high viral titers over 10^7 $TCID_{50}$/ml, as expected. Taking these results together, it seems that T-cells provide a shielding effect for the virus, as there are similar viral titers regardless if loaded cells were incubated with neutralizing serum or control serum.

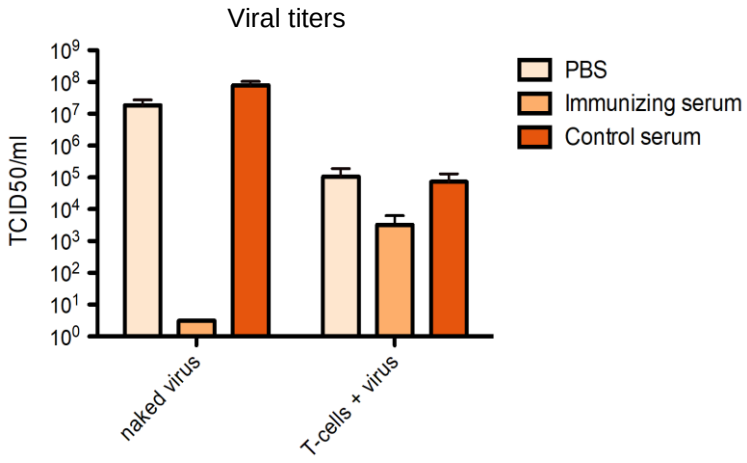

Figure 10: Potential shielding properties of candidate carrier cells

The viral titers of naked virus and virus loaded T-cells after incubation with neutralizing serum, control serum or PBS, respectively, are shown. T-cells were infected with rVSV-Luc at MOI 10 prior to the incubation. All samples were analyzed by $TCID_{50}$ assay for viral titers (Y-axis). Results show similar intracellular titers, whether the loaded T-cells were incubated with neutralizing serum, control serum or PBS, indicating a shielding effect of carrier cells. $TCID_{50}$/ml is plotted in log scale and values are expressed as mean and SD.

3.5 Viral progeny from infected T-cells can infect and replicate in target tumor cells

In order to determine whether VSV can be passed from infected T-cells to target tumor cells, a viral transfer assay was performed. 2 x 10^4 T-cells/sample were infected with rVSV-Luc at MOI 1 for one hour, washed with PBS, and then either cultured alone or co-cultured with ML2-wt tumor cells at a ratio of 1:10. As a control, tumor cells were directly infected with the same amount of virus that was applied to the T-cells. After 12 and 24 h p.i., supernatants were harvested and viral titers were measured by $TCID_{50}$ assay.

At early time points, results show only slight differences in viral titers in all samples whether T-cells where cultured alone or co-cultured with tumor cells. 12 hours p.i. viral titers in T-cells samples show 10^4 $TCID_{50}$/ml, while in co-cultured and control samples titers were around 10^5 $TCID_{50}$/ml. In contrast, after 24 h p.i., titers in the co-cultured sample were several logs higher than those achieved in T-cells alone. Titers at around 10^7 $TCID_{50}$/ml were measured, indicating that viral progeny could be released from infected T-cells and be transferred to susceptible target tumor cells, where it could replicate effectively.

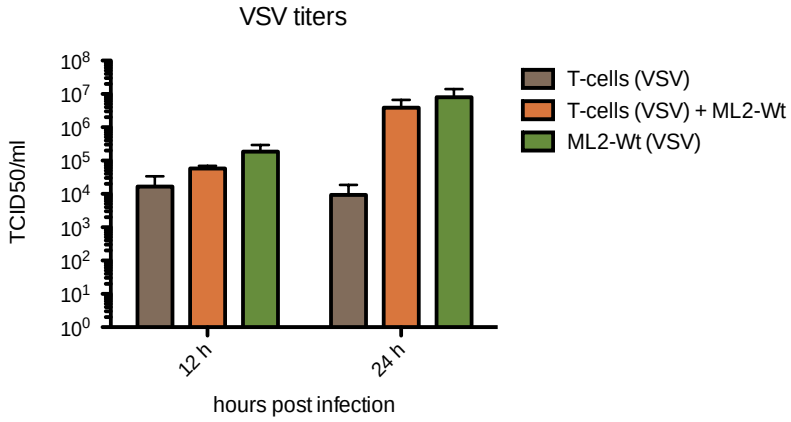

Figure 11: Released viral progeny can be transferred and replicate in target tumor cells

$TCID_{50}$ assay for viral titers in the supernatant of rVSV-Luc infected T-cells, either cultured alone or co-cultured with ML2-wt at a ratio of 1:10 (Y-axis), at different time points (X-axis) is shown. Control samples were infected with same amount of virus as that applied to the T-cells at t = 0. $TCID_{50}$/ml is plotted in log scale, and values are expressed as mean and SD. Data are representative for three individual experiments.

3.6 Co-cultivation of VSV-loaded TCR transgenic T-cells with target tumor cells results in tumor cell lysis

In order to determine if a potentially synergistic effect in tumor cell lysis could be achieved via combination therapy with transduced T-cells and VSV, an *in vitro* co-cultivation assay was performed. Several experiments with modifications to the protocol, regarding the infection procedure and effector-to-target (E:T) ratios, were carried out in order to optimize the conditions. The tumor cells (ML2-B7) were incubated with TCR transduced (generated by AG Krackhardt) or untransduced T-cells, either loaded with virus (rVSV-Luc) or uninfected, at different effector-to-target ratios. The supernatants were collected at various timepoints and stored at -80 °C for further analysis. For all experiments, flow cytometry analysis of tumor cell viability was performed by following the protocol as described above. ML2-B7 cells could be detected by their stably transduced GFP expression.

3.6.1 Experiment 1: Co-cultivation of VSV-infected transduced T-cells with target tumor cells

The experiment was performed under the following conditions: 4 x 10^4 transduced or untransduced T-cells/sample were infected with rVSV-Luc at MOI 1 for one hour at RT, washed thoroughly and then co-cultured with different amounts of tumor cells according to the following effector:target (E:T) ratios: 1:1, 1:5, 1:10 for 24 hours. Subsequently, cells were prepared for FACS analysis following the previously described staining protocol, and supernatants were kept for further analysis.

The TCR transduced T-cells, when co-cultured with their target ML2-B7 cells, showed high efficacy in tumor cell killing with nearly 100% of lysed tumor cells achieved when cultured in 1:1 ratio, and 40% and 30% for 1:5 and 1:10 ratios, respectively. When compared to infected, transduced samples, no additional effect could be seen. On the contrary, for low E:T ratios in those samples, the percentage of dead tumor cells is slightly lower with 30% in 1:5 ratio and 25% in 1:10. The infected but untransduced T-cells also resulted in efficient tumor cell killing, but to a lesser extent. In 1:1 ratio, 65% of tumor cells were found dead, and for 1:5 and 1:10 ratios, 14% and 17%, respectively. For untransduced, uninfected samples the percentage of dead tumor cells ranged between 12% and 17% among all ratios.

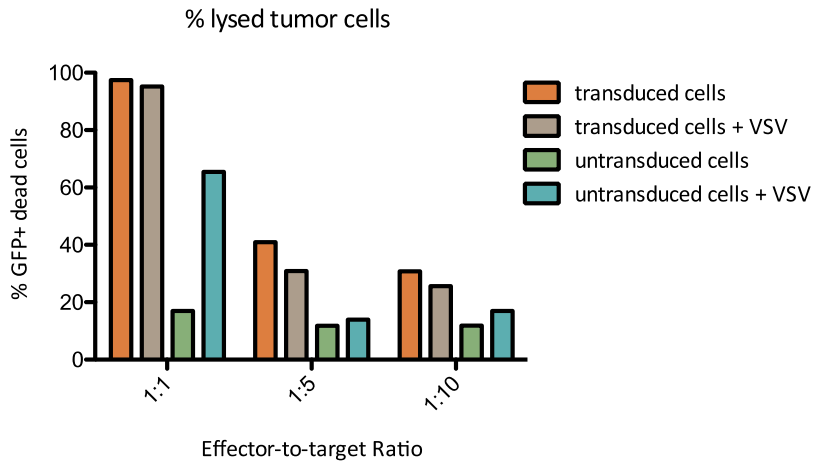

Figure 12:Co-cultivation of VSV-infected transduced T-cells with target tumor cells

FACS analysis of co-cultivated samples. Tumor cells (ML2-B7) were incubated with transduced or untransduced T-cells, either with or without virus (rVSV-Luc), at different effector-to-target ratios. The percentage of dead tumor cells (Y-axis) is shown for different E:T ratios (X-axis) for different combinations of co-cultivation.

3.6.2 Experiment 2: Co-cultivation with optimized infection protocol

Because we were unable to demonstrate an additive effect of virus infection to the T-cell mediated tumor cell toxicity in the previous experiment, we attempted to optimize the infection protocol and experimental conditions in a follow-up experiment. A pre-infection with rVSV-Luc at MOI 1 of the T-cells (4 x 10^4 cells/sample) was performed 16 h before co-cultivation to allow time for the virus to amplify within the T cells before activation by the tumor cells, which we hypothesized could inhibit virus replication through IFN-γ secretion. Subsequently, either infected or uninfected T-cells were transferred to different amounts of ML2-B7 tumor cells (Effector-to-target ratios: 1:2.5, 1:5, 1:10). As a control, ML2-wt cells were incubated with infected, transduced T-cells. After 24 h of incubation, supernatants were harvested and stored for further analysis in a -80 °C freezer, while cells were prepared for FACS analysis, following the protocol above.

Two individual experiments were carried out under these conditions, but great variability was observed among the two data sets (Figure 13). While transduced T-cells in A) showed nearly no effect in tumor cell killing, in B) the TCR transgenic T cells resulted in around 30% lysed tumor cells when applied in 1:2.5 and 1:5 ratio and 10% in 1:10 ratio. However, no significant difference in tumor cell lysis between infected and uninfected transduced T-cells could be observed. For infected, untransduced samples and infected, transduced T-cells co-cultured with control tumor cells, the best lytic effect could be seen with up to 60% dead tumor cells for 1:2.5 ratio, but then decreased with lower E:T ratios. This can be at least partly explained by the lack of IFN-γ production in those samples (Figure 14), which allows a more effective viral replication. The uninfected, untransduced samples resulted in less than 5% tumor cell death. When compared to the uninfected, transduced sample in A) no difference could be observed.

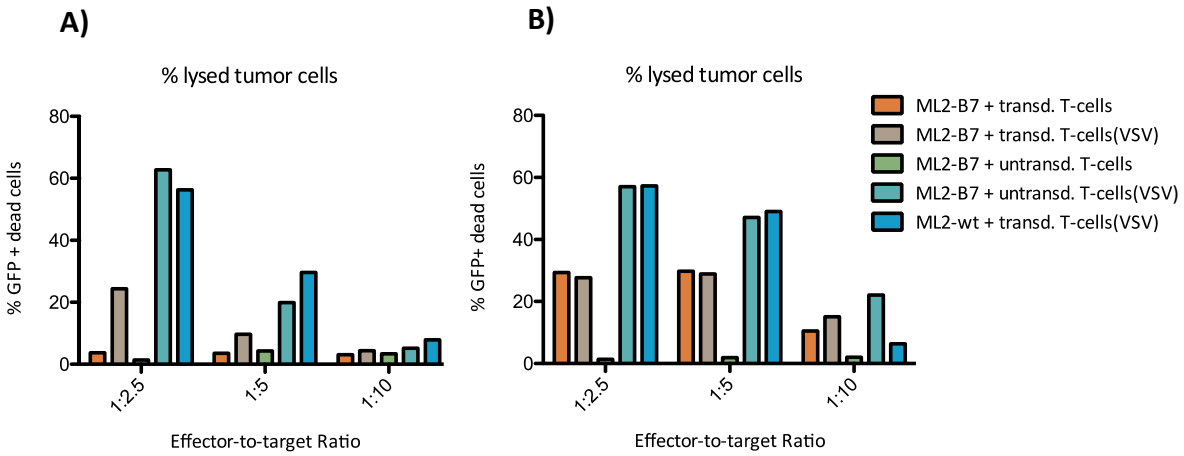

Figure 13: Co-cultivation of two separate experiments with revised infection protocol

FACS analysis of co-cultivated samples. Tumor cells (ML2-B7) were incubated with TCR transduced or untransduced T-cells, either with or without virus (rVSV-Luc), at different effector-to-target ratios. **A)** and **B)** Percentage of dead tumor cells (Y-axis) is shown for different E:T ratios (X-axis) for different combinations of co-cultivation. The data in A) and B) represent two individual experiments performed using T-cells derived from two separate donors.

3.6.2.1 VSV-infected T-cells maintained their ability to become activated upon stimulation with target tumor cells

To determine the activation status of the T-cells, the IFN-γ levels were measured in the supernatants of all samples from the experiments depicted in Figure 13 by ELISA assay. TCR transduced and also infected, transduced samples, when co-cultured with ML2-B7 cells show very high levels of IFN-γ production, with concentrations of up to nearly 9,000 pg/ml as seen in Figure 14B. In Figure 14A, the IFN-γ production was less effective, with maximal concentrations of around 4,000 pg/ml at a ratio of 1:2.5, which decreased at lower ratios to around 3,000 and 1,500 pg/ml, respectively. This correlates with the lower percentage of tumor cell killing as seen in Figure 13. However, no significant difference between infected and uninfected transduced samples could be observed, indicating that the infection with rVSV-Luc neither interferes with their ability to become activated upon stimulation with target tumor cells, nor results in a nonspecific stimulation of the cells. For untransduced cells, whether infected or not, and control samples, no significant level of IFN-γ production could be observed.

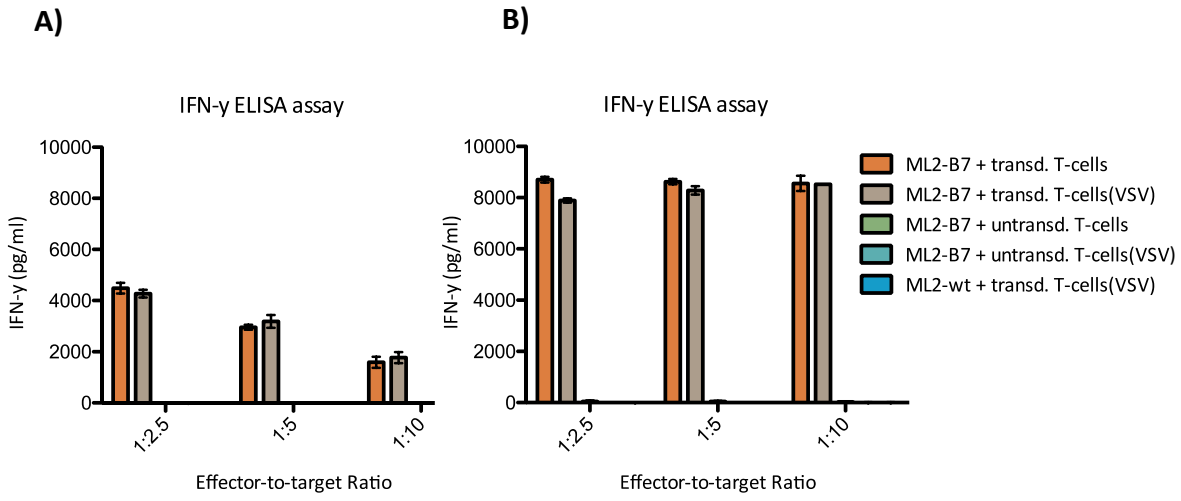

Figure 14: Analysis of activation status by measuring INF-γ concentration in supernatants

IFN-γ ELISA assay of supernatants obtained from co-cultured samples. Concentration of IFN-γ is shown in pg/ml (Y-axis) for different effector-to-target ratios (X-axis) for all co-cultured samples. Means of triplicate samples with SD are shown.

3.6.3 Experiment 3: Co-cultivation with revised effector-to-target ratios

Next, a co-cultivation experiment was performed in which the effector-to-target ratios were modified, while the infection procedure was performed under the same conditions as in the previous experiment. Therefore, the tumor cell number was kept fixed over all ratios, but the T-cell numbers were reduced to achieve the desired ratios. Again, T-cells were infected with rVSV-Luc at MOI 1, 16 hours prior to co-cultivation. 2 x 10^5 tumor cells/sample were plated, and different amounts of T-cells (4 x 10^4, 2 x 10^4, 1 x 10^4 for E:T ratios: 0.2:1, 0.1:1, 0.05:1, respectively) were added. As a control, ML2-wt were incubated with infected, TCR transduced T-cells. After 24 h of incubation, supernatants were harvested and stored for further analysis at -80 °C, while cells were prepared for FACS analysis, following the protocol above.

Again, two separate experiments under the same conditions were carried out, but this time, the results were consistent among the two data sets, and the trend was comparable to that observed in the previous experiment. Transduced T-cells were again very effective in killing tumor cells, with an average of 73% lysed cells achieved for the 0.2:1 ratio, but the effect decreased to around 45% and 25% at E:T 0.1:1 and 0.05:1, respectively. This time, infected transduced samples show an even higher percentage of dead tumor cells over all ratios, and especially for lower ratios, the difference is more appreciable, although not statistically significant (unpaired t-test: $p = 0.075$). In 0.1:1 and 0.05:1 infected, transduced samples were able to kill 65% and 45% of tumor cells, respectively. However, the best lytic effect could be seen in infected, untransduced samples with a slight decrease over the ratios from 90% to 70%. Uninfected, untransduced samples show steady percentage of dead cells at around 20% over all ratios investigated.

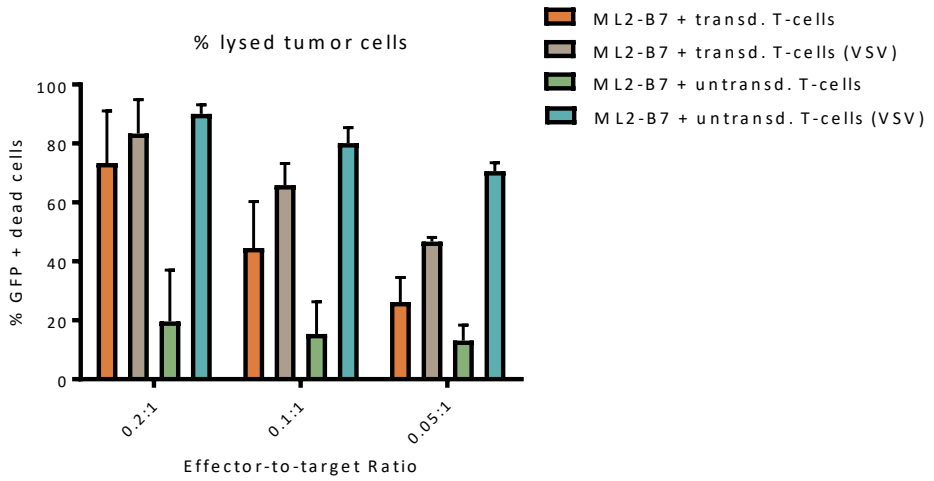

Figure 15: Co-cultivation with modified effector-to-target ratios

FACS analysis of co-cultivated samples. Tumor cells (ML2-B7) were incubated with transduced or untransduced T-cells, either with or without virus (rVSV-Luc), at different effector-to-target ratios. The percentage of dead tumor cells (Y-axis) is shown for different E:T ratios (X-axis) for different combinations of co-cultivation. Mean + SD of two individual experiments is plotted.

Again, the activation status of co-cultured T-cells in the above experiment was determined via IFN-γ ELISA assay. Transduced T-cells, when co-cultured with ML2-B7 tumor cells, produced very high IFN-γ concentrations up to 13,000 pg/ml when cultured in a 0.2:1 ratio, with a linear decrease to around 8,000 pg/ml with increasing ratios (Figure 16A). The same trend was observed for infected, transduced samples. In contrast, the untransduced samples demonstrated no significant IFN-γ production.

Next, the supernatants of co-cultured infected samples were subjected to $TCID_{50}$ assay in order to measure viral titers. The highest titers could be observed in untransduced samples with up 1 x 10^8 $TCID_{50}$/ml, regardless of E:T ratio. Similar titers were achieved in control samples in which the tumor cells did not express the targeted B7 antigen. However, titers were reduced for transduced T-cell samples to around 5 x 10^6 $TCID_{50}$/ml.

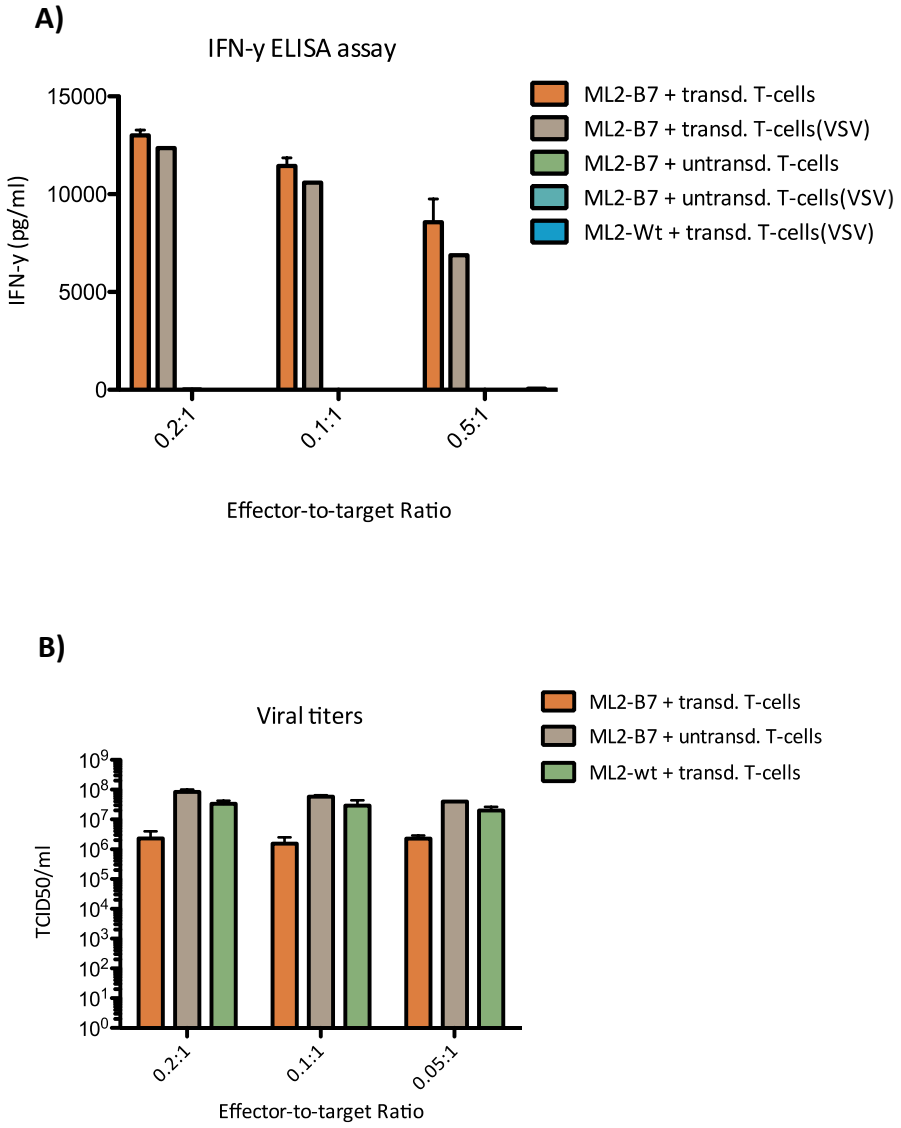

Figure 16: Analysis of INF-γ and viral titers in supernatants

A) IFN-γ ELISA assay of supernatants from co-cultured samples. Concentrations of IFN-γ were determined by ELISA assay and are shown in pg/ml (Y-axis) for different effector-to-target ratios (X-axis) for all co-cultured samples. **B)** $TCID_{50}$ assay for viral titers in the supernatant of rVSV-Luc infected T-cells co-cultured with tumor cells (Y-axis) at different effector-to-target ratios (X-axis). $TCID_{50}$/ml is plotted in log scale, and values of two individual experiments are expressed as mean + SD.

4 Discussion

Virotherapy and adoptive T-cell therapy have both already shown great success in modern tumor therapy. Recently, many years of intensive research have finally paid off – in the field of oncolytic virus therapy, as well as in immunotherapy, new approaches have found their way into the clinic. An engineered herpes simplex virus received FDA approval in 2015 for the use in advanced melanoma (Coffin 2016). Being the first approved treatment of its kind in the western world, hopes have been raised that the approval of other, and potentially improved, virus-based therapies may soon follow. The field of immunotherapy is also emerging as an important weapon in the fight against cancer. In particular, adoptive T-cell therapy has already shown great success in clinical trials and excitingly, in August 2017 an FDA approval for CAR T-cell therapy was released (Prasad 2017). A recent clinical trial demonstrated the efficacy of this therapy in refractory B-cell acute lymphoblastic leukemia (ALL) in children. Preliminary data showed that remission occurred in 83% of all young patients (Grupp, Laetsch et al. 2016). However, severe side effects should be considered, and especially the cytokine release syndrome (CRS) and neurological events could be life-threatening (Namuduri and Brentjens 2016). Despite its enormous success in hematological malignancies, solid tumors seem to be a greater challenge for T-cell therapy. A major obstacle is to identify a suitable antigen that would serve as a target for the engineered T-cells. As solid tumors normally express a huge variation of antigens due to biological heterogeneity, it is hard to identify one perfect target that is fitting for all (Yeku, Li et al. 2017). When treating a solid tumor, the combination therapy with oncolytic virus might provide an advantage, as nearly every tumor cell is susceptible to OV therapy. This can compensate for the challenge of tumor immune escape, such as antigen loss, drift, and shift associated with T-cell therapy targeting a single antigen. Also, OVs could mediate polyclonal antitumor immune responses that help to destroy cancer cells which evade direct viral infection. Nevertheless, systemic delivery of oncolytic virus therapies faces considerable challenges, and therefore, transgenic T-cells might offer a novel solution as an ideal vehicle, as well as an additional therapeutic agent.

Overall, virotherapy and immunotherapy both have many advantages to offer, as well as barriers that limit their full success in tumor therapy. We hypothesized that a combination of the two approaches would provide several benefits and help to overcome the limitations of each. As our group has already thoroughly characterized oncolytic VSV as a cancer therapeutic for HCC, it was a logical candidate for preliminary experiments in this study. VSV has shown promising results in HCC models (Ebert, Shinozaki et al. 2003, Shinozaki, Ebert et al. 2004, Shinozaki, Ebert et al. 2005), and it represents a promising vector for *in vivo* experiments, as it is a replication-competent virus, and therefore, efficient spread of virus through the tumor mass and high levels of oncolysis compared to non-replicating vectors can be achieved (Kirn, Martuza et al. 2001). Our collaborating group (Prof. Dr. med. Krackhardt) established techniques to generate TCR transgenic T cells against several TAAs in a humanized system. As a proof of principle, we decided to work with an acute myeloid leukemia cell line and a TCR construct that recognizes myeloperoxidase expressed by those cells. The transduced tumor cells and TCR transgenic T-cells were kindly provided by AG Krackhardt. III. Med., Klinikum rechts der Isar.

VSV has inherent tumor selectivity and therefore is able to replicate freely in a wide range of tumor cells. Nevertheless, preliminary experiments were needed in order to investigate the potential of VSV to replicate in our candidate tumor cells. Our data show that VSV is able to replicate efficiently in ML2-wt and ML2-B7 cells with titers of up to 10^8 $TCID_{50}$/ml. Also, the replication kinetics demonstrate a rapid propagation of virus, as the titers already increase as early as 6 hours post infection.

The tumor selectivity of VSV is attributed to defects in IFN signalling pathways in tumor cells that occur during malignant transformation (Stojdl, Lichty et al. 2000). In many cancerous cells the type I interferon pathway, normally inducing antiviral response, is impaired. Because VSV is extremely sensitive to the antiviral actions of IFN, the virus is substantially attenuated in healthy tissue, while being able to replicate in and destroy tumor cells. As a preliminary experiment to determine the sensitivity of our target tumor cells to VSV-mediated oncolysis, we investigated the response of the tumor cells to type I IFN. The results showed that ML2-wt and ML2-B7 cells are not sensitive to type I IFN. High viral titers could be achieved whether the cells were treated or not treated with interferon. While virus yields over 10^7 $TCID_{50}$/ml could be measured in supernatants of cells pretreated with

low IFN concentrations, in higher concentrations titers were only slightly reduced. Also, we show that the retroviral transduction of tumor cells does not alter the responsiveness to interferon, as no differences between the transduced versus untransduced cells could be observed. Taken together, our target tumor cells are susceptible to VSV due to impaired IFN signalling pathways. The pretreatment with interferon failed to protect the cells, and VSV is able to replicate effectively in ML2-wt and ML2-B7 cells, indicating that this model is suitable for our proposed therapy.

Next, preliminary experiments to monitor the fate of human T-cells after infection with VSV were performed. Our aim was to establish a protocol with the best inoculating dose of virus and incubation time that would lead to the highest T-cell loading efficacy. For these optimization experiments, we decided to work with untransduced T-cells in order to avoid higher expenses. Also, different donors were chosen for every experiment to estimate inherent variability of the infection kinetics. The FACS analysis of GFP and 7AAD live/dead staining revealed that untransduced T-cell were able to support infection by rVSV-GFP in a time- and dose-responsive manner. For MOI 0.1, at an early phase of infection, an increasing amount of infected, living cells could be already be observed, peaking after 36 hours p.i. with nearly 18% of GFP+ living cells. For the intermediate MOI of 1, the peak was reached earlier, with 30% of infected living T-cells after 24 hours. For MOI 10, the highest percentage was already observed after 16 hours p.i., amounting to 27% of GFP+ living cells. With ongoing infection, the amount of dead cells accumulated for all MOIs and raised to high numbers over 60% after 48 hours. In contrast, uninfected cells (MOI 0) do not lead to an increase in cell death over the time-points analyzed, indicating that the loss of cell viability was, in fact, due to the rVSV-GFP infection.

Looking at Figure 8, it becomes clear that there is variability in the susceptibility of different donors to virus infection. Despite applying the same infection protocol for all experiments, the maximum T-cell loading efficacy for MOI 1 after 24 hours ranged between 17% and 35%. One experiment even showed up to 40% infected living cells for MOI 10 at an early time point. Interestingly, we observed that high proliferation rates of the T cells prior to the start of the experiment correlated directly with high levels of infection. One possible explanation is that VSV replication in lymphocytes is cell cycle dependent. This hypothesis is supported by a study of Oliere et al. that reveals that VSV replicates effectively in activated

primary T-lymphocytes, while in resting cells, viral protein synthesis was not detectable (Oliere, Arguello et al. 2008). This also explains the high levels of infected cells we were able to achieve. Normally, healthy T-cells are not very permissive to VSV replication, but our protocol for T-cell enrichment includes an activation step with human IL2 and CD3/CD28 Dynabeads® prior to their use in experiments. Hence, the cells are proliferating quite well and become more susceptible to VSV infection. Nevertheless, the higher levels of infected cells at early time-points lead to a larger population of dead T-cells at subsequent time-points. This is an important consideration, in that, in order to achieve the maximum synergistic effects, it is crucial that the T-cells survive long enough in circulation in order to reach the tumor site prior to lysis, as well as to maintain T-cell viability to achieve sufficient cytotoxic effector functions. Therefore the ideal scenario would be to choose the optimal infection conditions to achieve the highest percentage of infected cells without sacrificing T-cell viability, especially during the first 24 hours, as it is estimated that T-cells need at least 24 hours to reach the tumor site *in vivo*. Based on these criteria, we have chosen an MOI of 1 as the ideal amount of VSV for infection of T-cells, and this condition was used in all subsequent experiments.

As a next step, we investigated the effect of virus infection on T-cell functionality. In order to determine the activation status of the cells, we measured concentrations of IFN-γ in the supernatants using an IFN-γ ELISA assay. In addition to our samples, we included a positive control consisting of T cells that were reactivated overnight with CD3/CD28 beads prior to the experiment as seen in Figure 9A. The results show a linear increase of IFN-γ in the supernatants over time for uninfected control T-cells from approximately 100 pg/ml up to 300 pg/ml. This suggests a constant IFN-γ secretion accumulating in the medium over time. Similarly, for rVSV-GFP infected T-cells, the same trend was observed for all MOIs without any significant changes, suggesting that the infection of T-cells does not alter their activation status. For MOI 10, the IFN-γ concentrations were slightly reduced compared to others, which likely is the consequence of the fact that a high percentage of these cells died due to virus-mediated cell lysis, beginning at early time points. In contrast to our experimental T-cells samples, the positive control cells that were freshly reactivated, showed values over 1200 pg/ml INF-γ in the supernatant. This helps to support the hypothesis that T-cells do not become activated upon infection with rVSV-GFP, as the IFN-γ values were much lower compared to the reactivated controls. Unfortunately, it was not possible to

include a negative control, because of an intrinsic activation step in our T-cell enrichment protocol. Our finding here, stands in contrast to a study by Qiao et al., where the loading of rVSV-MΔ51 onto OT-I CD8+ T-cells led to an enhanced T-cell function and activity *in vitro* measured by an augmented interferon release (Qiao, Wang et al. 2008). However, it is important to note that rVSV-MΔ51 is engineered to induce antiviral IFN expression in normal cells, which could be an explanation for the high levels of IFN-γ secreted by OT-I T-cells after infection.

The kinetics of rVSV-GFP replication in each sample was determined by $TCID_{50}$ assay from conditioned supernatants. The results demonstrate an increase over time from 5×10^5 to 5×10^7 $TCID_{50}$/ml for MOI 0.1 and a constant $TCID_{50}$/ml value between 10^7 and 5×10^7 for MOI 1 and 10, respectively. However, especially for high MOIs a decrease of viral titers after 48 hours was detected. The trend, whether increasing or being steady over time, correlates with the FACS data (Figure 7). For the low MOI, the replication peaked 36 h p.i., when the highest GFP+ cell counts were observed by FACS. For higher MOIs, by 16 h p.i., large populations of GFP+ living cells were observed, which is consistent with the high $TCID_{50}$/ml values at this early time point.

Since the sample T-cells were thoroughly washed after infection in this experiment, and therefore the majority of free virus particles should have been removed from supernatants, we can infer that the measured titers of rVSV-GFP in the supernatant is a direct reflection of virus production by the cells. Also, for all MOIs, the concentrations of virus measured in the supernatants were higher than the starting concentrations of 3×10^4 (MOI 0.1), 3×10^5 (MOI 1) and 3×10^6 (MOI 10), respectively, indicating that replication had indeed taken place.

Our next aim was to investigate the potential benefits provided by a combination of oncolytic virotherapy with TCR transgenic T-cells. We hypothesized that loading oncolytic virus onto T-cells would improve virus delivery, as VSV could be protected against neutralizing blood components within carrier cells while trafficking to the tumor site. To test this, we established an *in vitro* protection assay, where rVSV-Luc infected T-cells were either incubated with neutralizing serum, control serum or PBS and afterwards subjected to $TCID_{50}$ assay for measuring intracellular viral titers. Results showed that similar viral titers could be

achieved, whether the infected cells were incubated with neutralizing serum or not. Values around 10^5 $TCID_{50}$/ml could be observed for loaded cells treated with PBS or control serum, while titers after treatment with neutralizing serum were reduced by 1 log. In contrast, total inactivation of naked VSV after incubation with neutralizing serum was observed. However, it is important to note, that the design of our experiment is slightly biased, because free virus samples could not be washed as the loaded cells were, prior to measuring viral titers, and therefore, neutralizing serum is still present during the titration on BHK-21 cells. Thus, it would not be correct to compare titers between loaded cell samples and naked virus samples, but rather, we should consider naked virions incubated with neutralizing serum as a positive control, indicating that the serum is effectively neutralizing VSV. For future experiments, the experimental design would need to be further modified to include an extra step in our protocol. Instead of a washing step, the inactivation of neutralizing components in the serum after incubation could be considered. For this purpose, the addition of trypsin might be a good option as it is able to digest neutralizing antibodies (Walmsley, Rudnick et al. 2013). However, additional tests would be necessary in order determine whether trypsin could have an effect on the virus itself.

When comparing viral titers of loaded T-cells and naked virus samples in the absence of neutralizing antibodies, a noticeable difference could be seen. This gap can be explained by the infection procedure: While the applied concentration of virus is the same in both cases, as we have demonstrated in previous experiments, the infection of T cells is rather inefficient, and a substantial portion of the viral particles added were likely not associated with T cells and were, therefore, washed away in the subsequent washing step. This is a very probable explanation for the marked reduction in titers in infected T cells compared to the amount of input virus. Regardless, despite the presence of neutralizing antibodies, loaded T-cells showed similar intracellular viral titers when compared to those incubated with control serum or PBS treated cells. An *in vivo* study by Power et al. supports our findings, by showing that a cell-mediated systemic delivery of VSV to the tumor site was effective, while viral titers were not detectable after injection of naked virus to mice in the presence of circulating antiviral antibodies (Power, Wang et al. 2007). Moreover, Ong et al. previously described that T-cells infected with oncolytic measles virus were protected when exposed to different dilutions of measles immune serum, while cell-free virus was inactivated (Ong, Hasegawa et al. 2007). The shielding properties obtained by cellular carriers address

one of the major obstacles to overcome, as for successful systemic virotherapy, repeat dosing will likely be necessary, and therefore, production of neutralizing antiviral antibodies in patients will occur.

But what is the fate of oncolytic virus once it has arrived safely at the tumor site? Our next experiment focused on determining whether the virus could be transferred from infected T-cells and become available for replication in the more permissive target tumor cells. We set up a viral transfer assay, meaning that loaded T-cells were co-cultured with ML2-wt, and supernatants were subjected to $TCID_{50}$ assay for measuring viral titers after an incubation period. As a positive control, tumor cells were directly infected with the same amount of naked virus at the starting point of co-cultivation. Results showed that, after 24 hours, viral titers in supernatants of the co-cultivated samples were several logs higher than those achieved in T-cells alone. Infected T-cells showed titers of around 10^4 $TCID_{50}$/ml, while in co-cultured and control samples titers increased to 10^7 $TCID_{50}$/ml. Hence, co-cultured samples induced an increase of viral titers far above the initial amount of virus, indicating that VSV leads to infection and effective replication in target tumor cells. However, it is not clear if the infection is only due to released virus that was synthesized de novo by the carrier T-cells or also a result of virus particles that just adhered on their cell surface. Qiao et al. demonstrated in a similar set up, that the infection of target tumor cells could be still observed, even if loaded OT-I cells were not in direct contact with those cells. Despite using a trans-well membrane for separation of the co-cultured cells, infection of B16 tumor cells was still observed, but at lower levels compared to direct cell contact in co-cultivation. This indicates that, at least, a portion of the infection of tumor cells is the consequence of the direct release of virus from the T-cells (Qiao, Wang et al. 2008). Additionally, a recent study by VanSeggelen et al. supports our results. They demonstrate that, after co-cultivation of VSV-loaded CAR T-cells with D2F2 tumor cells, a drastic increase of viral titer was observed, indicating that virus transfer occurred, and amplification in target cancerous cells took place (VanSeggelen, Tantalo et al. 2015).

Unfortunately, it is difficult to investigate the hypothesized homing ability of TCR transgenic T-cells to the tumor site *in vitro*. Nevertheless, preliminary experiments with TCR transgenic T-cells, either infected with VSV or not, were performed in order to monitor potential synergistic effects in tumor cell lysis when co-cultured with their target tumor cells. How-

ever, the first experiments did not reveal promising results: Because transduced T-cells showed a very high efficacy in tumor cell killing, with up to nearly 100% when applied at a 1:1 ratio, no additional effect in cell lysis could be observed by loading VSV onto T-cells prior to co-cultivation. In samples with lower E:T ratios, the same trend was observed, but with a lower percentage of killed tumor cells. A possible reason for those results could be attributed to the infection procedure, as co-cultivation followed directly after the T-cells were infected. Therefore, there was no opportunity for the virus to expand prior to activation of the transduced T-cells upon incubation with their target tumor cells, which leads to high levels of IFN-γ production (Figure 14). This cytokine release by activated T-cells could be counterproductive to this combination treatment modality. As viral titers were reduced in samples of TCR transduced cells compared to untransduced ones (Figure 16B), we speculated that IFN-γ has antiviral actions. It was previously reported, that IFN-γ release by immune cells plays an important role in the clearance of virus infection. In particular, Kokordelis et al. describe this mechanism for hepatitis C infection (Kokordelis, Kramer et al. 2014). Additionally, the findings by Jo et al. support our hypothesis: In an *in vitro* experiment, they demonstrated that IFN-γ is able to block viral replication in a dose-dependent manner. Further, they pointed out the importance of noncytolytic virus inhibition mediated by IFN-γ release by virus-specific CD8+ T-cells (Jo, Aichele et al. 2009).

In order to better optimize the experimental setup, a modified infection protocol was established. We decided to pre-infect the T-cells for 16 hours prior to co-cultivation in order to allow time for viral replication in the absence of cytokines that are produced in the co-culture. Indeed, viral titers achieved using this infection protocol were 2 to 3 logs higher compared those in the previous experiment (data not shown), although transduced cells still generally produced lower levels overall. As seen in Figure 13B, again no increase in tumor cell lysis in the infected TCR T-cell co-cultures, compared to uninfected, could be observed. Also, one out of the two replicate experiments produced unexpected results, in that nearly no lytic effect in uninfected, transduced T-cells could be detected. This could be due to an ineffective activation upon stimulation with the target tumor cells in this experiment. An IFN-γ ELISA assay partially explained our findings, as the level of IFN-γ production was drastically different in the two experiments (Figure 14A and B). While concentrations of up to 9000 pg/ml could be achieved in samples in which effective tumor cell killing was observed, only 4000 pg/ml of IFN-γ were detected in samples with inefficient lysis of tumor

cells in 1:2.5 ratios. IFN-γ levels also decreased drastically with lower E:T ratios, while in the experiment with effective elimination of tumor cells, high IFN-γ concentrations were achieved over all ratios. Together, these findings suggest that the efficacy of tumor cell lysis correlates directly with levels of IFN-γ production and, therefore, with the activation status of the T-cells. Moreover, we demonstrated that no change in activation status occurred when T-cells were infected with rVSV-Luc. As seen in Figure 14A and 16A, similar or slightly reduced concentrations of IFN-γ were measured whether transduced T-cells were infected or not. This indicates that VSV-infected transduced T-cells preserve their ability to become activated upon stimulation with target tumor cells. In contrast, no significant concentrations of IFN-γ were detected when untransduced T-cells or control cells were co-cultured with tumor cells.

In a next optimization step, the preparation of varying ratios of effector to target cells was modified. This time, the amount of tumor cells was kept constant, while the number of T-cells was reduced respectively to achieve the desired ratios. Our rationale for this change was, that the detection of a potential additional effect provided by the virus would be enabled, as the total number of T-cells was kept to a minimum. Also, by maintaining a constant amount of tumor cells, the comparison among the different samples would be more straightforward. Once more, TCR transduced T-cells resulted in effective tumor cell killing with an average percentage of 73% lysed cells in 0.2:1 ratio, decreasing to 44% and 26% for E:T ratios of 0.1:1 and 0.05:1, respectively. Encouragingly, in this experimental setup, transduced T-cells loaded with rVSV-Luc demonstrated enhanced antitumor effects. Infected, transduced samples were able to achieve 83%, 65% and 46% of lysed tumor cells for decreasing E:T ratios, respectively. Although, the results were not statistically significant, an appreciable trend could be observed. Probably a larger number of experiments would be necessary in order to achieve significance in this context. Additionally, optimized E:T ratios could further improve the antitumor effects of a combination therapy. It would be beneficial to further decrease the amount of TCR T-cells, as this represents a more realistic situation with less IFN-γ production, allowing the virus to replicate and lyse tumor cells to a larger extent. However, the best lytic effect was achieved by infected, untransduced T-cells, ranging between 70% and 90% of killed tumor cells over the ratios. This effect could also be seen in a control group, where infected transduced T-cells were co-cultured with ML2-wt (Figure 13). This is likely due to the lack of IFN-γ production in those samples,

therefore allowing effective viral replication and cell lysis. As shown in Figure 16B, viral titers in samples with no detectable IFN-γ production were as high as 10^8 $TCID_{50}$/ml, while in transduced samples, the titers were reduced to around 5 x 10^6 $TCID_{50}$/ml. Nevertheless, we have to keep in mind that this *in vitro* experiment does not completely represent a realistic *in vivo* situation. In this artificial setting, the T-cells are in direct contact with the tumor cells, and the ability of TCR transgenic T-cells versus control T-cells to home to the tumor is not considered. Therefore, while VSV-infected untransduced T-cells showed the best results here, it would not be possible to reproduce this in a living organism, as these T-cells would likely arrive at a low frequency to the tumor site. Furthermore, the effect of IFN-γ and its inhibition of viral replication might be exaggerated in our *in vitro* testing. The experimental setup was performed in a very small total volume, and therefore, the virus was exposed to very high concentrations of IFN-γ, which might not be comparable to those achieved *in vivo*. Another point to consider is that the effect of TCR T-cells might be overestimated because of very high antigen presentation in this setting due to the close proximity of effector to target cells. However, in a clinical setup, T-cell monotherapies might struggle because of heterogenous antigen presentation and the predominant immunosuppressive tumor microenvironment. Therefore, in this setting, a combination with oncolytic VSV would be more easily appreciated compared to T-cell therapy alone.

Once more, supernatants of co-cultured samples were subjected to IFN-γ ELISA assay in order to monitor their activation status. Again, we were able to observe very high concentrations of IFN-γ of up to 13,000 pg/ml in samples co-cultured at a 0.2:1 ratio, which decrease at lower ratios to around 8,000 pg/ml. Also for VSV-infected transduced samples the same trend could be observed. Here we show that levels of IFN-γ correlate with the number of lysed tumor cells. Looking at Figure 15A and 16A, it becomes clear that higher amounts of killed tumor cells can be observed when higher concentrations of IFN-γ are released by transduced T-cells, whether infected or not. Again, reduced viral titers in transduced T-cell samples that were co-cultured with their target tumor cells could be observed, probably due to the high IFN-γ production in those samples, when compared to control T-cells (Figure 16B). However, reduced viral titers might provide a safety mechanism in a translational setting that could prevent the patient from the onset of viremia.

In summary, we demonstrated in various *in vitro* experiments that TCR transgenic T-cells might be ideal carriers for oncolytic VSV. However, in these limited *in vitro* studies, we were not able to investigate the important role of the immune system and its influence on a potential combination therapy. The fully intact immune system represents a double-edged sword, as on the one hand it hinders the full success of oncolytic virotherapy by inhibiting viral replication, but on the other hand it boosts antitumor efficacy by attracting immune cells to the tumor site and generating a pro-inflammatory microenvironment. Furthermore, there will always be a fine line between the balance of antiviral immune responses, on the one hand being important for safety, and on the other hand playing an inhibitory role to the direct oncolytic effect of viruses. Therefore, cancer therapeutics aiming to use oncolytic viruses, particularly in immunotherapeutic applications, should carefully consider the implications of immune modulation.

5 Conclusion

Our study represents a step forward in the optimization of the promising field of modern tumor therapy, as both oncolytic virotherapy and adoptive T-cell therapy already found their ways into the clinic. We now hypothesized that a combination of both approaches would enhance the efficacy of both components by overcoming the limitations and hurdles of each. The systemic delivery of viruses faces limited efficacy due to rapid clearance by components of the immune system, while circulating through the bloodstream. Therefore the use of cellular carriers to chaperone oncolytic viruses might be the ideal way to overcome this challenge. In particular, to utilize T-cell receptor (TCR) transgenic T-cells as vehicles represents an appealing strategy, as they deliver oncolytic virus directly to tumors expressing the target antigen. Besides providing a delivery mechanism through specific homing to the tumor site, carrier cells offer shielding properties and also possess a direct antitumor effector function themselves, allowing additive therapeutic effects with virotherapy.

In this proof-of-principle study, we show that human T-cells offer great potential to serve as cellular carriers for oncolytic VSV, as they allow effective viral replication and transfer to the target tumor cells. Moreover, we demonstrated a substantial shielding effect in the presence of antiviral antibodies by our candidate carrier cells that might empower them to chaperone OV safely through the systemic circulation. TCR transgenic T-cells and oncolytic VSV both function as potent antitumor agents as evidenced by a substantial tumor cell lysis in co-cultivation. Although a combination of both approaches resulted in enhanced tumor cell elimination, the effect was not statistically significant. Nevertheless, the trend observed is encouraging and would justify the application to further *in vivo* investigations allowing a more realistic setup with heterogenous antigen presentation to exclude a possible overestimation of antitumor effects by TCR T-cells. Supportively, co-cultivation revealed that VSV infection did not alter the activation status of T-cells, as evidenced by IFN-γ production, and transduced T-cells maintained their cytotoxic effector function.

Overall, the use of TCR transgenic T-cells as cellular carriers could provide a promising new strategy for improving tumor therapy by enriching the local concentration of virus at the

tumor site, leading to optimized direct oncolytic effects, as well as by presenting themselves as a powerful weapon against cancer due to antitumor effector functions.

5.1 Outlook

Taken together, our preliminary experiments of loading oncolytic virus onto antigen-specific T-cells show promising results and further investigations are warranted. Next steps would include *in vivo* experiments to examine the capacity of T-cells to chaperone virus to tumor sites and to monitor the spread and viral replication within the tumors. Furthermore, animal models would allow an analysis of how systemic virotherapy influences adoptive T-cell therapy and the other way round. Therefore, the potential for additive or synergistic therapeutic effects could be investigated. As this study was performed in a model system for testing the proof-of-principle, another crucial step for further investigations would be the application to more challenging models of solid tumors such as HCC. Therefore, the establishment of HCC TAA-specific TCR transgenic T-cells would be necessary in order to investigate whether a combination therapy leads to enhanced antitumor effects in the treatment of liver cancer. Although the isolation, expansion, and generation of TAA-specific T-cells would be challenging, the addition of a simple pre-incubation step with oncolytic virus would offer great potential for improved tumor therapy.

6 References

1. Alemany, R., K. Suzuki and D. T. Curiel (2000). "Blood clearance rates of adenovirus type 5 in mice." J Gen Virol **81**(Pt 11): 2605-2609.

2. Altomonte, J., R. Braren, S. Schulz, S. Marozin, E. J. Rummeny, R. M. Schmid and O. Ebert (2008). "Synergistic antitumor effects of transarterial viroembolization for multifocal hepatocellular carcinoma in rats." Hepatology **48**(6): 1864-1873.

3. Altomonte, J., S. Marozin, E. N. De Toni, A. Rizzani, I. Esposito, K. Steiger, A. Feuchtinger, C. Hellerbrand, R. M. Schmid and O. Ebert (2013). "Antifibrotic properties of transarterial oncolytic VSV therapy for hepatocellular carcinoma in rats with thioacetamide-induced liver fibrosis." Mol Ther **21**(11): 2032-2042.

4. Altomonte, J., K. A. Munoz-Alvarez, K. Shinozaki, C. Baumgartner, G. Kaissis, R. Braren and O. Ebert (2016). "Transarterial Administration of Oncolytic Viruses for Locoregional Therapy of Orthotopic HCC in Rats." J Vis Exp(110).

5. Barnett, F. H., N. G. Rainov, K. Ikeda, D. E. Schuback, P. Elliott, C. M. Kramm, M. Chase, N. H. Qureshi, G. t. Harsh, E. A. Chiocca and X. O. Breakefield (1999). "Selective delivery of herpes virus vectors to experimental brain tumors using RMP-7." Cancer Gene Ther **6**(1): 14-20.

6. Benencia, F., M. C. Courreges, J. R. Conejo-Garcia, R. J. Buckanovich, L. Zhang, R. H. Carroll, M. A. Morgan and G. Coukos (2005). "Oncolytic HSV exerts direct antiangiogenic activity in ovarian carcinoma." Hum Gene Ther **16**(6): 765-778.

7. Breitbach, C. J., R. Arulanandam, N. De Silva, S. H. Thorne, R. Patt, M. Daneshmand, A. Moon, C. Ilkow, J. Burke, T. H. Hwang, J. Heo, M. Cho, H. Chen, F. A. Angarita, C. Addison, J. A. McCart, J. C. Bell and D. H. Kirn (2013). "Oncolytic vaccinia virus disrupts tumor-associated vasculature in humans." Cancer Res **73**(4): 1265-1275.

8. Cattaneo, R., T. Miest, E. V. Shashkova and M. A. Barry (2008). "Reprogrammed viruses as cancer therapeutics: targeted, armed and shielded." Nat Rev Microbiol **6**(7): 529-540.

9. Chen, H. H., R. Cawood, Y. El-Sherbini, L. Purdie, M. Bazan-Peregrino, L. W. Seymour and R. C. Carlisle (2011). "Active adenoviral vascular penetration by targeted formation of heterocellular endothelial-epithelial syncytia." Mol Ther **19**(1): 67-75.

10. Coffin, R. (2016). "Interview with Robert Coffin, inventor of T-VEC: the first oncolytic immunotherapy approved for the treatment of cancer." Immunotherapy **8**(2): 103-106.

11. Critchley-Thorne, R. J., D. L. Simons, N. Yan, A. K. Miyahira, F. M. Dirbas, D. L. Johnson, S. M. Swetter, R. W. Carlson, G. A. Fisher, A. Koong, S. Holmes and P. P. Lee (2009). "Impaired interferon signaling is a common immune defect in human cancer." Proc Natl Acad Sci U S A **106**(22): 9010-9015.

12. Diaz, R. M., F. Galivo, T. Kottke, P. Wongthida, J. Qiao, J. Thompson, M. Valdes, G. Barber and R. G. Vile (2007). "Oncolytic immunovirotherapy for melanoma using vesicular stomatitis virus." Cancer Res **67**(6): 2840-2848.

13. Dudley, M. E. and S. A. Rosenberg (2003). "Adoptive-cell-transfer therapy for the treatment of patients with cancer." Nat Rev Cancer **3**(9): 666-675.

14. Ebert, O., K. Shinozaki, T. G. Huang, M. J. Savontaus, A. Garcia-Sastre and S. L. Woo (2003). "Oncolytic vesicular stomatitis virus for treatment of orthotopic hepatocellular carcinoma in immune-competent rats." Cancer Res **63**(13): 3605-3611.

15. Ebert, O., K. Shinozaki, C. Kournioti, M. S. Park, A. Garcia-Sastre and S. L. Woo (2004). "Syncytia induction enhances the oncolytic potential of vesicular stomatitis virus in virotherapy for cancer." Cancer Res **64**(9): 3265-3270.

16. Everts, B. and H. G. van der Poel (2005). "Replication-selective oncolytic viruses in the treatment of cancer." Cancer Gene Ther **12**(2): 141-161.

17. Garber, K. (2006). "China approves world's first oncolytic virus therapy for cancer treatment." J Natl Cancer Inst **98**(5): 298-300.

18. Garnock-Jones, K. P. (2016). "Talimogene Laherparepvec: A Review in Unresectable Metastatic Melanoma." BioDrugs **30**(5): 461-468.

19. Gong, J., E. Sachdev, A. C. Mita and M. M. Mita (2016). "Clinical development of reovirus for cancer therapy: An oncolytic virus with immune-mediated antitumor activity." World J Methodol **6**(1): 25-42.

20. Grupp, S. A., T. W. Laetsch, J. Buechner, H. Bittencourt, S. L. Maude, M. R. Verneris, G. D. Myers, M. W. Boyer, S. Rives, B. De Moerloose, E. R. Nemecek, K. Schlis, P. L. Martin, M. Qayed, P. Bader, H. Hiramatsu, F. Mechinaud, G. A. Yanik, C. Peters, A. Biondi, A. Baruchel, N. Boissel, J. Krueger, C. H. June, K. Sen, Y. Zhang, K. E. Thudium, P. A. Wood, T. Taran and M. A. Pulsipher (2016). "Analysis of a Global Registration Trial of the Efficacy and Safety of CTL019 in Pediatric and Young Adults with Relapsed/Refractory Acute Lymphoblastic Leukemia (ALL)." Blood **128**(22): 221-221.

21. Guo, Z. S., Z. Liu and D. L. Bartlett (2014). "Oncolytic Immunotherapy: Dying the Right Way is a Key to Eliciting Potent Antitumor Immunity." Front Oncol **4**: 74.

22. Hastie, E., M. Cataldi, I. Marriott and V. Z. Grdzelishvili (2013). "Understanding and altering cell tropism of vesicular stomatitis virus." Virus Res **176**(1-2): 16-32.

23. Hastie, E. and V. Z. Grdzelishvili (2012). "Vesicular stomatitis virus as a flexible platform for oncolytic virotherapy against cancer." J Gen Virol **93**(Pt 12): 2529-2545.

24. Jenks, N., R. Myers, S. M. Greiner, J. Thompson, E. K. Mader, A. Greenslade, G. E. Griesmann, M. J. Federspiel, J. Rakela, M. J. Borad, R. G. Vile, G. N. Barber, T. R. Meier, M. C. Blanco, S. K. Carlson, S. J. Russell and K. W. Peng (2010). "Safety studies on intrahepatic or intratumoral injection of oncolytic vesicular stomatitis virus expressing interferon-beta in rodents and nonhuman primates." Hum Gene Ther **21**(4): 451-462.

25. Jo, J., U. Aichele, N. Kersting, R. Klein, P. Aichele, E. Bisse, A. K. Sewell, H. E. Blum, R. Bartenschlager, V. Lohmann and R. Thimme (2009). "Analysis of CD8+ T-cell-mediated inhibition of hepatitis C virus replication using a novel immunological model." Gastroenterology **136**(4): 1391-1401.

26. Johnson, L. A., R. A. Morgan, M. E. Dudley, L. Cassard, J. C. Yang, M. S. Hughes, U. S. Kammula, R. E. Royal, R. M. Sherry, J. R. Wunderlich, C. C. Lee, N. P. Restifo, S. L. Schwarz, A.

P. Cogdill, R. J. Bishop, H. Kim, C. C. Brewer, S. F. Rudy, C. VanWaes, J. L. Davis, A. Mathur, R. T. Ripley, D. A. Nathan, C. M. Laurencot and S. A. Rosenberg (2009). "Gene therapy with human and mouse T-cell receptors mediates cancer regression and targets normal tissues expressing cognate antigen." Blood **114**(3): 535-546.

27. Kershaw, M. H., J. A. Westwood and P. K. Darcy (2013). "Gene-engineered T cells for cancer therapy." Nat Rev Cancer **13**(8): 525-541.

28. Kirn, D., R. L. Martuza and J. Zwiebel (2001). "Replication-selective virotherapy for cancer: Biological principles, risk management and future directions." Nat Med **7**(7): 781-787.

29. Klar, R., S. Schober, M. Rami, S. Mall, J. Merl, S. M. Hauck, M. Ueffing, A. Admon, J. Slotta-Huspenina, M. Schwaiger, S. Stevanovic, R. A. Oostendorp, D. H. Busch, C. Peschel and A. M. Krackhardt (2014). "Therapeutic targeting of naturally presented myeloperoxidase-derived HLA peptide ligands on myeloid leukemia cells by TCR-transgenic T cells." Leukemia **28**(12): 2355-2366.

30. Kokordelis, P., B. Kramer, C. Korner, C. Boesecke, E. Voigt, P. Ingiliz, A. Glassner, M. Eisenhardt, F. Wolter, D. Kaczmarek, H. D. Nischalke, J. K. Rockstroh, U. Spengler and J. Nattermann (2014). "An effective interferon-gamma-mediated inhibition of hepatitis C virus replication by natural killer cells is associated with spontaneous clearance of acute hepatitis C in human immunodeficiency virus-positive patients." Hepatology **59**(3): 814-827.

31. Kottke, T., F. Galivo, P. Wongthida, R. Maria Diaz, J. Thompson, D. Jevremovic, G. N. Barber, G. Hall, J. Chester, P. Selby, K. Harrington, A. Melcher and R. G. Vile (2008). "Treg Depletion-enhanced IL-2 Treatment Facilitates Therapy of Established Tumors Using Systemically Delivered Oncolytic Virus." Mol Ther **16**(7): 1217-1226.

32. Lichty, B. D., C. J. Breitbach, D. F. Stojdl and J. C. Bell (2014). "Going viral with cancer immunotherapy." Nat Rev Cancer **14**(8): 559-567.

33. Lichty, B. D., A. T. Power, D. F. Stojdl and J. C. Bell (2004). "Vesicular stomatitis virus: re-inventing the bullet." Trends Mol Med **10**(5): 210-216.

34. Lyles, D. S. and C. E. Rupprecht (2007). Rhabdoviridae, in Fields virology. Philadelphia, Wolters Kluwer Health/Lippincott Williams & Wilkins.

35. Marchini, A., E. M. Scott and J. Rommelaere (2016). "Overcoming Barriers in Oncolytic Virotherapy with HDAC Inhibitors and Immune Checkpoint Blockade." Viruses **8**(1).

36. Marozin, S., J. Altomonte, K. A. Munoz-Alvarez, A. Rizzani, E. N. De Toni, W. E. Thasler, R. M. Schmid and O. Ebert (2015). "STAT3 inhibition reduces toxicity of oncolytic VSV and provides a potentially synergistic combination therapy for hepatocellular carcinoma." Cancer Gene Ther **22**(6): 317-325.

37. Morgan, R. A., M. E. Dudley, J. R. Wunderlich, M. S. Hughes, J. C. Yang, R. M. Sherry, R. E. Royal, S. L. Topalian, U. S. Kammula, N. P. Restifo, Z. Zheng, A. Nahvi, C. R. de Vries, L. J. Rogers-Freezer, S. A. Mavroukakis and S. A. Rosenberg (2006). "Cancer regression in patients after transfer of genetically engineered lymphocytes." Science **314**(5796): 126-129.

38. Munguia, A., T. Ota, T. Miest and S. J. Russell (2008). "Cell carriers to deliver oncolytic viruses to sites of myeloma tumor growth." Gene Ther **15**(10): 797-806.

39. Namuduri, M. and R. J. Brentjens (2016). "Medical management of side effects related to CAR T cell therapy in hematologic malignancies." Expert Rev Hematol **9**(6): 511-513.

40. Neri, D. and R. Bicknell (2005). "Tumour vascular targeting." Nat Rev Cancer **5**(6): 436-446.

41. Oliere, S., M. Arguello, T. Mesplede, V. Tumilasci, P. Nakhaei, D. Stojdl, N. Sonenberg, J. Bell and J. Hiscott (2008). "Vesicular stomatitis virus oncolysis of T lymphocytes requires cell cycle entry and translation initiation." J Virol **82**(12): 5735-5749.

42. Ong, H. T., K. Hasegawa, A. B. Dietz, S. J. Russell and K. W. Peng (2007). "Evaluation of T cells as carriers for systemic measles virotherapy in the presence of antiviral antibodies." Gene Ther **14**(4): 324-333.

43. Power, A. T. and J. C. Bell (2007). "Cell-based delivery of oncolytic viruses: a new strategic alliance for a biological strike against cancer." Mol Ther **15**(4): 660-665.

44. Power, A. T., J. Wang, T. J. Falls, J. M. Paterson, K. A. Parato, B. D. Lichty, D. F. Stojdl, P. A. Forsyth, H. Atkins and J. C. Bell (2007). "Carrier cell-based delivery of an oncolytic virus circumvents antiviral immunity." Mol Ther **15**(1): 123-130.

45. Prasad, V. (2017). "Immunotherapy: Tisagenlecleucel - the first approved CAR-T-cell therapy: implications for payers and policy makers." Nat Rev Clin Oncol.

46. Qiao, J., H. Wang, T. Kottke, R. M. Diaz, C. Willmon, A. Hudacek, J. Thompson, K. Parato, J. Bell, J. Naik, J. Chester, P. Selby, K. Harrington, A. Melcher and R. G. Vile (2008). "Loading of oncolytic vesicular stomatitis virus onto antigen-specific T cells enhances the efficacy of adoptive T-cell therapy of tumors." Gene Ther **15**(8): 604-616.

47. Restifo, N. P., M. E. Dudley and S. A. Rosenberg (2012). "Adoptive immunotherapy for cancer: harnessing the T cell response." Nat Rev Immunol **12**(4): 269-281.

48. Robbins, P. F., R. A. Morgan, S. A. Feldman, J. C. Yang, R. M. Sherry, M. E. Dudley, J. R. Wunderlich, A. V. Nahvi, L. J. Helman, C. L. Mackall, U. S. Kammula, M. S. Hughes, N. P. Restifo, M. Raffeld, C. C. Lee, C. L. Levy, Y. F. Li, M. El-Gamil, S. L. Schwarz, C. Laurencot and S. A. Rosenberg (2011). "Tumor regression in patients with metastatic synovial cell sarcoma and melanoma using genetically engineered lymphocytes reactive with NY-ESO-1." J Clin Oncol **29**(7): 917-924.

49. Roy, D. G. and J. C. Bell (2013). "Cell carriers for oncolytic viruses: current challenges and future directions." Oncolytic Virother **2**: 47-56.

50. Russell, S. J., K. W. Peng and J. C. Bell (2012). "Oncolytic virotherapy." Nat Biotechnol **30**(7): 658-670.

51. Schuster, I. G., D. H. Busch, E. Eppinger, E. Kremmer, S. Milosevic, C. Hennard, C. Kuttler, J. W. Ellwart, B. Frankenberger, E. Nossner, C. Salat, C. Bogner, A. Borkhardt, H. J. Kolb and A. M. Krackhardt (2007). "Allorestricted T cells with specificity for the FMNL1-derived peptide PP2 have potent antitumor activity against hematologic and other malignancies." Blood **110**(8): 2931-2939.

52. Shinozaki, K., O. Ebert, C. Kournioti, Y. S. Tai and S. L. Woo (2004). "Oncolysis of multifocal hepatocellular carcinoma in the rat liver by hepatic artery infusion of vesicular stomatitis virus." Mol Ther **9**(3): 368-376.

53. Shinozaki, K., O. Ebert and S. L. Woo (2005). "Eradication of advanced hepatocellular carcinoma in rats via repeated hepatic arterial infusions of recombinant VSV." Hepatology **41**(1): 196-203.

54. Stojdl, D. F., B. Lichty, S. Knowles, R. Marius, H. Atkins, N. Sonenberg and J. C. Bell (2000). "Exploiting tumor-specific defects in the interferon pathway with a previously unknown oncolytic virus." Nat Med **6**(7): 821-825.

55. Tesfay, M. Z., A. C. Kirk, E. M. Hadac, G. E. Griesmann, M. J. Federspiel, G. N. Barber, S. M. Henry, K. W. Peng and S. J. Russell (2013). "PEGylation of vesicular stomatitis virus extends virus persistence in blood circulation of passively immunized mice." J Virol **87**(7): 3752-3759.

56. Thomas, E. D., S. Meza-Perez, K. S. Bevis, T. D. Randall, G. Y. Gillespie, C. Langford and R. D. Alvarez (2016). "IL-12 Expressing oncolytic herpes simplex virus promotes anti-tumor activity and immunologic control of metastatic ovarian cancer in mice." J Ovarian Res **9**(1): 70.

57. Toro Bejarano, M. and J. R. Merchan (2015). "Targeting tumor vasculature through oncolytic virotherapy: recent advances." Oncolytic Virother **4**: 169-181.

58. Underhill, D. M. and A. Ozinsky (2002). "Phagocytosis of microbes: complexity in action." Annu Rev Immunol **20**: 825-852.

59. VanSeggelen, H., D. G. Tantalo, A. Afsahi, J. A. Hammill and J. L. Bramson (2015). "Chimeric antigen receptor-engineered T cells as oncolytic virus carriers." Mol Ther Oncolytics **2**: 15014.

60. Walmsley, S. J., P. A. Rudnick, Y. Liang, Q. Dong, S. E. Stein and A. I. Nesvizhskii (2013). "Comprehensive analysis of protein digestion using six trypsins reveals the origin of trypsin as a significant source of variability in proteomics." J Proteome Res **12**(12): 5666-5680.

61. Weigand, L. U., X. Liang, S. Schmied, S. Mall, R. Klar, O. J. Stotzer, C. Salat, K. Gotze, J. Mautner, C. Peschel and A. M. Krackhardt (2012). "Isolation of human MHC class II-restricted T cell receptors from the autologous T-cell repertoire with potent anti-leukaemic reactivity." Immunology **137**(3): 226-238.

62. Workenhe, S. T., G. Simmons, J. G. Pol, B. D. Lichty, W. P. Halford and K. L. Mossman (2014). "Immunogenic HSV-mediated oncolysis shapes the antitumor immune response and contributes to therapeutic efficacy." Mol Ther **22**(1): 123-131.

63. Yeku, O., X. Li and R. J. Brentjens (2017). "Adoptive T-Cell Therapy for Solid Tumors." Am Soc Clin Oncol Educ Book **37**: 193-204.

64. Yotnda, P., A. R. Davis, M. J. Hicks, N. S. Templeton and M. K. Brenner (2004). "Liposomal enhancement of the antitumor activity of conditionally replication-competent adenoviral plasmids." Mol Ther **9**(4): 489-495.

7 Acknowledgements

Thanks to Prof. Dr. med. Oliver Ebert, who gave me the opportunity to work in his research group and to explore the stunning field of oncolytic virotherapy. He always could make some time to discuss appearing issues and came up with new approaches during the lab meetings.

I want to say a special thank you to Dr. rer. nat. Jennifer Altomonte, who had an open ear whenever I needed her and tried to help me, no matter how much work she had to do. With her never-ending optimism she encouraged me to go on and came up with new ideas and possible solutions over and over again.

Thanks to David Grunert, my patient lab partner who introduced me into the field of research. He showed me how to work in a proper scientific way and made me think outside the box. Also thanks for overlooking my mistakes during the first time.

Thanks to Sabine Mall and the AG Krackhardt, who provided me with the TCR transgenic T-cells and the tumor cell lines and all the required know-how about the cell handling, experimental set-up and analysis.

Thanks to my lovely lab members, Sarah Abdullahi and Arturo Lopez Martinez, for all those nice talks at any possible day- or night-time, that helped me to endure the hard working hours. Also thanks for sharing all the moments of happiness together when an experiment worked.

Finally, a big thank you goes to all my family and friends for their continuous support and encouragement they have given me throughout my study. It wouldn't have been possible without you!!